

**Ergodic Convergence Rates
of Markov Processes
—Eigenvalues, Inequalities
and Ergodic Theory**
(Volume V)

Mu-Fa Chen
(Beijing Normal University)

First Edition 2000
Second Edition 2009

Contents

Volume V

- [64] With Rong-Rong Chen. Top eigenpairs of large scale matrices. *SIAM Trans. Appl. Math.* 2022. 3(1): 1–25.1636
- [65] Hermitizable, isospectral matrices or differential operators. Chapter 3 in *Dirichlet Forms and Related Topics—In Honor of Masatoshi Fukushima’s Beiju 2022.* eds. Chen, Z.Q., Takeda, M., Uemura, T., 45–55. *Springer Proc. Math. & Statis.*, vol. 394.1662

Volume I

- [01] Coupling for jump processes, *Acta Math. Sin. New Ser.* 1986, 2:2, 123–136. 1
- [02] With S.F. Li, Coupling methods for multidimensional diffusion processes, *Ann. of Probab.* 1989, 17:1, 151-177. 14
- [03] Exponential L^2 -convergence and L^2 -spectral gap for Markov processes, *Math. Sin. New Ser.* 1991, 7:1, 19–37. 43
- [1] With F.Y. Wang, Application of coupling method to the first eigenvalue on manifold, *Sci. Sin.(A)* 1993, 23:11 (Chinese Edition), 1130-1140; 1994, 37:1 (English Edition), 1-14. 65
- [2] Optimal Markovian couplings and applications, *Acta Math. Sin. New Ser.* 1994, 10:3, 260-275. 82
- [3] Optimal couplings and application to Riemannian geometry, *Prob. Theory and Math. Stat.*, Vol. 1, Eds. B. Grigelionis et al, 1994 VPS/TEV, 121-142. 102
- [4] On the ergodic region of Schlögl’s model, in *Proceedings of International Conference on Dirichlet Forms and Stochastic Processes*, Edited by Z.M. Ma, M. Röckner and J.A. Yan, Walter de Gruyter Publishers, 1995, 87-102. 124
- [5] With F.Y. Wang, Estimation of the first eigenvalue of second order elliptic operators, *J. Funct. Anal.* 1995, 131:2, 345-363. 139
- [6] With F.Y. Wang, Estimates of logarithmic Sobolev constant, *J. Funct. Anal.* 1997, 144:2, 287-300. 156
- [7] Estimation of spectral gap for Markov chains, *Acta Math. Sin. New Series* 1996, 12:4, 337-360. 169
- [8] With F.Y. Wang, Estimation of spectral gap for elliptic operators, *Trans. Amer. Math. Soc.* 1997, 349:3, 1239-1267. 203
- [9] With F.Y. Wang, General formula for lower bound of the first eigenvalue on Riemannian manifolds, *Sci. Sin.* 1997, 27:1, 34–42 (Chinese Edition); 1997, 40:4, 384–394 (English Edition) 237
- [10] Trilogy of couplings and general formulas for lower bound of spectral gap, in “Probability Towards 2000”, Edited by L. Accardi and C. Heyde, *Lecture Notes in Statis.* **128**, 123–136, Springer-Verlag, 1998. 249
- [11] Coupling, spectral gap and related topics (I), *Chin. Sci. Bulletin*, 1997, 42:14, 1472–1477 (Chinese Edition); 1997, 42:16, 1321–1327 (English Edition). 262
- [12] Coupling, spectral gap and related topics (II), *Chin. Sci. Bulletin*, 1997, 42:15, 1585–1591 (Chinese Edition); 1997, 42:17, 1409–1416 (English Edition). 270

- [13] Coupling, spectral gap and related topics (III), Chin. Sci. Bulletin, 1997, 42:16, 1696–1703 (Chinese Edition); 1997, 42:18, 1497–1505 (English Edition). 279
- [14] Estimate of exponential convergence rate in total variation by spectral gap, Acta Math. Sin. Ser. (A) 1998, 41:1, 1–6; Acta Math. Sin. New Ser. 1998, 14:1, 9–16. 289
- [15] With F. Y. Wang, Cheeger’s inequalities for general symmetric forms and existence criteria for spectral gap. Abstract: Chin. Sci. Bulletin 1998, 43:14 (Chinese Edition), 1475–1477; 43:18 (English Edition), 1516–1519. Ann. Prob. 2000, 28:1, 235–257 305
- [16] Analytic proof of dual variational formula for the first eigenvalue in dimension one, Sci. in China (A) 1999, 29:4 (Chinese Edition), 327–336; 42:8 (English Edition), 805–815. 331
- [17] Nash inequalities for general symmetric forms, Acta Math. Sin. Eng. Ser. 1999, 15:3, 353–370. 348

Volume II

- [18] Equivalence of exponential ergodicity and L^2 -exponential convergence for Markov chains, Stoch. Proc. Appl. 2000, 87:2, 281–297 376
- [19] Logarithmic Sobolev inequality for symmetric forms, Sci. in China (A) 2000, 30:3 (Chinese Edition), 203–209; 43:6 (English Edition), 601–608. 399
- [20] A new story of ergodic theory, in “Applied Probability”, 25–34, eds. R. Chan et al., AMS/IP Studies in Advanced Mathematics, vol. 26, 2002. 411
- [21] Eigenvalues, inequalities and ergodic theory, Chin. Sci. Bulletin, 1999, 44:23 (In Chinese), 2465–2470; 2000, 45:9 (English Edition), 769–774. 424
- [22] Eigenvalues, inequalities and ergodic theory (II), Adv. in Math. (China) 1999, 28:6, 481–505. 432
- [23] The principal eigenvalue for jump processes, Acta Math. Sin. Eng. Ser. 2000, 16:3, 361–368 463
- [24] With Y.Z. Wang, Algebraic Convergence of Markov Chains, Ann. Appl. Prob. 2003, 13:2, 604–627 474
- [25] Explicit bounds of the first eigenvalue, Sci. China (A) 2000, 39:9 (Chinese Edition), 769–776; 43:10 (English Edition), 1051–1059 497
- [26] Variational formulas and approximation theorems for the first eigenvalue, Sci. China (A) 2001, 31:1 (Chinese Edition), 28–36; 44:4 (English Edition), 409–418 511

- [27] With E. Scacciatelli and L. Yao, Linear approximation of the first eigenvalue on compact manifolds, *Sci. China (A)* 2001, 31:9 (Chinese Edition), 807–816; 2002 (English Edition), 45:4, 450–461 535
- [28] With Y.H. Zhang and X.L. Zhao, Dual Variational Formulas for the First Dirichlet Eigenvalue on Half-Line, *Sci. China (A)* 2003, 33:4 (Chinese Edition), 371–383; (English Edition), 46:6, 847–861 551
- [29] Ergodic Convergence Rates of Markov Processes — Eigenvalues, Inequalities and Ergodic Theory, in Proceedings of “ICM 2002”, Vol. III, 41–52, Higher Education Press, Beijing 574
- [30] Variational formulas of Poincaré-type inequalities in Banach spaces of functions on the line, *Acta Math. Sin. Eng. Ser.* 2002, 18:3, 417–436 587
- [31] Variational formulas of Poincaré-type inequalities for birth-death processes, *Acta Math. Sin. Eng. Ser.* 2003, 19:4, 625–644 615
- [32] Variational formulas and explicit bounds of Poincaré-type inequalities for one-dimensional processes, *IMS Lecture Notes – Monograph Series*, Volume 41, 81–96 640
- [33] Ten explicit criteria of one-dimensional processes, *Advanced Studies in Pure Mathematics*, Vol. 39, 89–114, 2004, Mathematical Society of Japan 656
- [34] Capacitary criteria for Poincaré-type inequalities, *Potential Analysis* 2005, 23:4, 303–322 677
- [35] Exponential convergence rate in entropy, *Front. Math. China* 2007, 2:3, 329–358 696
- [36] Spectral gap and logarithmic Sobolev constant for continuous spin systems, *Acta Math. Sin. New Ser.* 2008, 24:5, 705–736 728

Volume III

- [37] Speed of stability for birth–death processes, *Front. Math. China* 2010, 5:3, 379–515 768
- [38] Basic estimates of stability rate for one-dimensional diffusions, Chapter 6 in “Probability Approximations and Beyond”, 75–99, *Lecture Notes in Statistics 205*, eds. A.D. Barbour, H.P. Chan and D. Siegmund, 2012 900
- [39] General estimate of the first eigenvalue on manifolds, *Front. Math. China* 2011, 6(6): 1025–1043 924
- [40] Lower bounds of the principal eigenvalue in dimension one, *Front. Math. China* 2012, 7(4): 645–668 947

- [41] Mixed principal eigenvalues in dimension one, *Front. Math. China* 2013, 8(2): 317–343 970
- [42] Bilateral Hardy-type inequalities, *Acta Math. Sin. Eng. Ser.* 2013, 29:1, 1–32 1017
- [43] The optimal constant in Hardy-type inequalities, *Acta Math. Sin. Eng. Ser.* 2015, 1063
- [44] Progress on Hardy-type inequalities, Chapter 7 in the book “Festschrift Masatoshi Fukushima”, 131–142. Eds: Z.Q. Chen, N. Jacob, M. Takeda, and T. Uemura, World Sci. 2015 1092
- [45] Mixed eigenvalues of discrete p -Laplacian, *Front. Math. China* 2014, 9(6): 1261–1292 1104
- [46] Mixed eigenvalues of p -Laplacian, *Front. Math. China* 2015, 1162

Volume IV

- [47] With Y.H. Zhang. Unified representation of formulas for single birth processes. *Front. Math. China* 2014, 9(4): 761–796. 1207
- [48] With X. Zhang. Isospectral operators. *Communications in Mathematics and Statistics* 2014, 2(1):17–32. 1243
- [49] Criteria for discrete spectrum of 1D operators. *Commun. Math. Stat.* 2014, 2(3): 279–309. 1259
- [50] Practical criterion for uniqueness of Q -processes. *Chinese Journal of Applied Probability and Statistics* 2015, 31(2): 213–224. 1289
- [51] Unified speed estimation of various stabilities (extended abstract). In: *Souvenir Booklet of the 24th International Workshop on Matrices and Statistics (25-28 May 2015)*, Haikou City, Hainan, China. Ed. Jeffrey J. Hunter. *Special Matrices* 2016; 4: 9–12. 1302
- [52] Unified speed estimation of various stabilities. *Chinese Journal of Applied Probability and Statistics* 2016; 32(1), 1–22. 1308
- [53] Efficient initials for computing the maximal eigenpair. *Front. Math. China* 2016, 11(6): 1379–1418. 1329
- [54] The charming leading eigenpair. *Advances in Mathematics (China)* 2017, 46(4): 281–297. 1370
- [55] Global algorithms for maximal eigenpair. *Front. Math. China* 2017, 12(5): 1023–1043. 1389
- [56] Trilogy on computing maximal eigenpair, in “Queueing Theory and Network Applications”, LNCS 10591: 312–329. Springer 2017 1411

- [57] Efficient algorithm for principal eigenpair of discrete p -Laplacian. Front. Math. China 2018, 13(3): 509–524. 1429
- [58] Hermitizable, isospectral complex matrices or differential operators. Front. Math. China 2018, 13(6): 1267–1311. 1445
- [59] With Li, Yue-Shuang. Development of powerful algorithm for maximal eigenpair. Front. Math. China 2019, 14(3): 493–519. 1492
- [60] With Li, Yue-Shuang. Improved global algorithms for maximal eigenpair. Front. Math. China 2019, 14(6): 1077–1116. 1520
- [61] On spectrum of Hermitizable tridiagonal matrices. Front. Math. China 2020, 15(2): 285–303. 1561
- [62] With Li, Jin-Yu. Hermitizable, isospectral complex second-order differential operators. Front. Math. China 2020, 15(5): 867–889. 1580
- [63] With Jia, Zhi-Gang, Pang, Hong-Kui. Computing top eigenpairs of Hermitizable matrix. Front. Math. China 2021, 16 (2): 345–379. . 1600

Top Eigenpairs of Large Scale Matrices

Mu-Fa Chen^{1,2,*} and Rong-Rong Chen³

¹RIMS, Jiangsu Normal University, Xuzhou, 221116, China;

²School of Mathematics and Key Laboratory of Mathematics, Beijing Normal University, Beijing 100875, China;

³Department of Electrical and Computer Engineering, University of Utah, UT 84112, USA.

December 20, 2020

Abstract

This paper is devoted to the study of an extended global algorithm on computing the top eigenpairs of a large class of matrices. Three versions of the algorithm are presented that includes a preliminary version for real matrices, one for complex matrices, and one for large scale sparse real matrix. Some examples are illustrated as powerful applications of the algorithms. The main contributions of the paper are two localized estimation techniques, plus the use of a machine learning inspired approach in terms of a modified power iteration. Based on these new tools, the proposed algorithm successfully employs the inverse iteration with varying shifts (a very fast “cubic algorithm”) to achieve a superior estimation accuracy and computation efficiency to existing approaches under the general setup considered in this work.

1 Introduction. Extended global algorithm

The top eigenpairs of matrix play an important role in many fields. In particular, for the maximal eigenpair for instance, there are well-known algorithms in several different fields. For web-search, it is called PageRank. For economic optimization, there is so called left-positive eigenvector method (cf. [1; Chapter 10]). For statistics, there is principal component analysis (abbrev. PCA) which is also used in quantum mechanics computation (quantum chemistry in

Received 22 December, 2021; Accepted 16 January, 2022

2020 *Mathematics Subject Classifications.* 15A18, 65F15.

Key words and phrases. matrix eigenpair, extended global algorithm, localized estimation technique, top eigenpair, large sparse matrix.

*Corresponding author. *Email address:* mfchen@bnu.edu.cn (M.-F. Chen), rchen@utah.edu (R.-R. Chen)

<http://www.global-sci.org/csiam-am>

©202x Global-Science Press

particular) and AI. In the last case, one needs not only the maximal one, but also a couple of the subsequent eigenpairs. Certainly, for such a well-developed field, there are some powerful algorithms in common use, the “singular value decomposition” (abbrev. SVD) for PCA for example. However, as mentioned at the beginning of [9; p.65, §2.6]: “In some cases, SVD will not only diagnose the problem, it will also solve it, in the sense of giving you a useful numerical answer, although, as we shall see, *not necessarily ‘the’ answer that you thought you should get.*” This happens for a number of known algorithms (see [7; Example 1] for instance) and so more careful study is valuable.

This paper is motivated by the study on the global algorithms given in [3, 7], where some effective algorithms were presented for computing the maximal eigenpair of a rather larger class of matrices. Roughly speaking, two approaches are adopted there: the power iteration (abbrev. PI) and the inverse power iteration with varying/fixed shifts (abbrev. IPI_v/IPI_f). The PI has only a little restriction on the initial vector and so has a wide range of applications. It is also economical (having lower computational complexity), but has a quite slow convergence speed, especially near the target eigenvalue. The fast convergence speed of the algorithms given in [3, 7] is mainly due to the use of IPI_v (having higher computational complexity). It is however quite dangerous if the initial is not close enough (from above) to the target eigenvalue. The last problem was avoided in [3, 7] mainly due to the assumption: the off-diagonal elements of the matrix are all nonnegative. This is essential: it implies the existence of the maximal eigenpair (as an application of the Perron–Frobenius theorem, by a shift if necessary). Then we have some important variational formulas for the upper/lower bounds of the maximal eigenvalue, i.e., the Collatz–Wielandt (abbrev. C-W) formula (cf. [2; §1 and Corollary 12]). For nonnegative matrix, the formula takes the following form:

$$\sup_{x>0} \min_k \frac{(Ax)(k)}{x(k)} = \lambda = \inf_{x>0} \max_k \frac{(Ax)(k)}{x(k)},$$

where λ is the maximal eigenvalue of the matrix A and $x(k)$ is the k th component of the vector x . The upper bound in the formula is very important in using IPI_v for avoiding the pitfalls (cf. [4; §4]). Now, a challenge appears:

Question: What can we do without the assumption of the nonnegative property of the off-diagonal elements?

A typical model led to the question is PCA, for which some of the off-diagonal elements can be negative. The question is quite serious since almost each advantage introduced in the previous paragraph is lost. We do not have the Perron–Frobenius theorem; more seriously, we do not have the C-W formula; and furthermore, the IPI_v is not practical.

Certainly, the answer to the above question is not obvious. If you have luckily produced enough courage, you may look for a way to find a substitute of the C-W formula. Assume that the given matrix A is real. Assume also

for a moment that the maximal eigenvalue λ we are working is positive. Of course, at the present case, the corresponding eigenvector g is not necessarily positive, and it may have negative or zero components. Because we are now bare-handed, to find an exit from the darkness, we have to go back to the original position: all we know is the eigenequation:

$$Ag = \lambda g. \quad (1)$$

That is, g is an eigenvector corresponding to the eigenvalue λ of A . It follows that once $g(k) \neq 0$, we must have $(Ag)(k)/g(k) > 0$, here we have preassumed that $\lambda > 0$. If a vector x produced by our iterative method (either PI or IPI) is close enough to g , then in one iteration, we have

$$x \approx g \implies Ax \approx Ag = \lambda g.$$

We now arrive at the first localized estimation technique: *check sign and locally bilateral estimates* (abbrev. CS-LBE). Due to the property given above, on the set

$$\mathcal{N}_x := \{k : |x(k)| > 0\}, \quad (2)$$

we should have

$$\frac{Ax}{x}(k) := \frac{Ax(k)}{x(k)} > 0, \quad k \in \mathcal{N}_x, \quad (3)$$

since $\lambda > 0$ by assumption. As usual, here “ $k \in \mathcal{N}_x$ ” means “for each $k \in \mathcal{N}_x$ ”. The procedure checking (3) is called “*check sign*” (abbrev. CS). Once this holds for a few of iterations, then we do not need to check it again, just continue the PI until the *relative difference* (abbrev. RD)

$$1 - \min_{k \in \mathcal{N}_x} \frac{Ax}{x}(k) \Big/ \max_{k \in \mathcal{N}_x} \frac{Ax}{x}(k) < \varepsilon \quad (4)$$

for some sufficiently small ε . Under condition $\lambda > 0$, assertions (3) and (4) are actually due to the convergence of PI, assuming for a moment that the maximal eigenvalue coincides with the maximal one in modulus. In practice, one has to take care for the initial vector in using PI to guarantee its convergence. Next, using condition $\lambda > 0$ again, by (3), we have

$$\text{either } (0 <) \frac{Ax}{x}(k) \leq \lambda \quad \text{or} \quad \frac{Ax}{x}(k) \geq \lambda \quad \text{for each } k \in \mathcal{N}_x.$$

Hence under condition (4) with $\varepsilon \ll 1$, we obtain the following *locally bilateral estimates* (abbrev. LBE):

$$(0 \leq) \min_{k \in \mathcal{N}_x} \frac{Ax}{x}(k) \leq \lambda \leq \max_{k \in \mathcal{N}_x} \frac{Ax}{x}(k), \quad (5)$$

the equalities in (5) hold once x is taken to be an eigenvector of the corresponding eigenvalue λ . We now regard (5) as a substitute of the C-W upper/lower estimates, and adopt

$$z := \max_{k \in \mathcal{N}_x} \frac{Ax}{x}(k) \quad (6)$$

as an upper bound of λ for the use in IPI_v or IPI_f . Condition (4) guarantees the validity of LBE (5) and then (6). Thus, in (3)–(6), we use only those x in a small neighborhood of the eigenvector of λ in the corresponding vector space. That is the meaning of “locally” used above.

In the above paragraph, we preassume that the maximal eigenvalue coincides with the one in modulus and is positive. This is important not only in computing the ratios above but also an essential point in the use of PI, since for which, the leading term in the algorithm is determined by the maximal eigenvalue in modulus, one cannot ignore the point “in modulus” here. Certainly, if one has known in advance that the spectrum (at least the top six eigenvalues) of A has satisfied the assumption, then the step we are working can be ignored. Otherwise, to remove the assumption, we simply use a *shift operator*: replacing A by

$$A_1 := A + \bar{\theta} I, \quad (7)$$

$$\bar{\theta} = \begin{cases} \theta & \text{if the order of } A \text{ is bigger than 6 and } \theta \text{ is an integer,} \\ \lceil \theta \rceil & \text{otherwise} \end{cases}$$

where $\lceil x \rceil$ denotes the minimal integer that is greater or equal to x , and the constant θ is an upper bound of the spectral radius. Here, the use of $\bar{\theta}$ instead of θ is to simplify the computation. Clearly, the spectrum of A_1 is nonnegative. Therefore, working on A_1 , the assumption just mentioned holds automatically. The reason that we choose the top six eigenpairs is to compare with the “eigs” package of MatLab, which is designed for the same aim (See section 4 below). Certainly, one can continue the algorithm for additional subsequent eigenpairs.

There are two ways to obtain an upper bound of the spectral radius of general complex matrix A without additional restriction. The first one is a theoretic result, deduced by the Gershgorin Circle Theorem (cf. [10]):

$$\theta = \min \{ \|A\|_\infty, \|A\|_1 \}, \quad \|A\|_\infty := \sup_i \sum_j |a_{ij}|, \quad \|A\|_1 = \|A^*\|_\infty$$

where A^* denotes the transpose of A . In the symmetric case, the two terms in $\{\dots\}$ are the same. The disadvantage of this method is that the result is usually quite rough. We now introduce the second numerical method which is similar to the technique deducing (1) – (6) above. Since we are now interested only in the modulus of the eigenvalue λ , instead of (1), we should start at

$$|Ag| = |\lambda| |g|.$$

Next, we follow the analysis between (1) and (6). The output x produced by PI, with suitable initial and after enough iterations, should have the following property. With the same \mathcal{N}_x defined by (2), replacing

$$\frac{Ax}{x} \quad \text{by} \quad \left| \frac{Ax}{x} \right|, \quad \lambda \quad \text{by} \quad |\lambda|, \quad \text{and} \quad z \quad \text{by} \quad \theta,$$

we obtain the analogs of (4) – (6) as follows:

$$\begin{aligned} 1 - \min_{k \in \mathcal{N}_x} \left| \frac{Ax}{x} \right|(k) / \max_{k \in \mathcal{N}_x} \left| \frac{Ax}{x} \right|(k) &< \varepsilon, \\ \min_{k \in \mathcal{N}_x} \left| \frac{Ax}{x} \right|(k) &\leq |\lambda| \leq \max_{k \in \mathcal{N}_x} \left| \frac{Ax}{x} \right|(k), \\ \theta &:= \max_{k \in \mathcal{N}_x} \left| \frac{Ax}{x} \right|(k). \end{aligned} \quad (8)$$

Starting from $\mathbf{1}/\|\mathbf{1}\|$, where $\mathbf{1}$ is the constant column vector having its component 1 everywhere and $\|x\|$ is the L_2 -norm of x . The resulting θ defined by (8) is what we need for (7). This method is especially good for PI, it converges economically to λ^* , the maximal eigenvalue in modulus, but not the real maximum, effective enough unless it is too close to λ^* . Hence this method is good enough for our purpose. The value of θ is noticeable since a larger θ makes the lower convergence speed of PI:

$$\lambda_1 > \lambda_2 > 0 \implies (0, 1) \ni \frac{\lambda_2 + \alpha}{\lambda_1 + \alpha} \uparrow \quad \text{as } \alpha (> 0) \uparrow.$$

We emphasize that the constant θ defined by (8) is used only in (7) for producing a matrix with nonnegative spectrum having positive six top eigenvalues. In the subsequent estimation of the eigenpairs, one does not use it again. In the special case that the given matrix already has the required property just mentioned above, one can simply ignore this shift procedure.

Usually, one needs to run the IPI_v only for a few of iterations since its convergence speed is very fast. Otherwise, the calculation will overflow quickly. The computation can be finished once the output arrives at the required precision level:

$$\max_{k \in \mathcal{N}_x} \frac{Ax}{x}(k) - \min_{k \in \mathcal{N}_x} \frac{Ax}{x}(k) < \varepsilon, \quad (9)$$

the left-hand part above is called the *amplitude of LBE*. If we do not want to compute the next eigenpair, then we can stop the computations here. If otherwise, one has to improve the precise level of the output of the eigenvector. For this, one should continue the work, using IPI_f instead of IPI_v . This is important since for computing the next eigenpairs, we will go to the subspace which is orthogonal to this eigenvector. The computation of orthogonalization often requires a higher level of precision. Failure to achieve such a precision often leads to error propagation and thus incorrect final results.

We now discuss the construction of the initial vector used by PI. First, for the maximal eigenpair, simply choose the *initial vector*

$$x_0 = \mathbf{1}/\|\mathbf{1}\|. \quad (10)$$

Once the computation of the maximal eigenpair is done, we obtain the first (maximal) eigenvector, say g_1 . After $k - 1$ steps, we have $k - 1$ eigenvectors

$\{g_1, \dots, g_{k-1}\}$ (normalized with respect to their L_2 -norm, respectively). Then the *initial vector* for computing the k th eigenpair can be chosen to be the projection vector of x_0 defined by (10) on the space which is orthogonal to $\text{Span}\{g_1, \dots, g_{k-1}\}$. In general, for a given linear space \mathcal{L} , let \mathcal{L}^\perp denote its orthogonal space. Then, the projection $\text{Proj}(x, k)$ of a vector x on the space $\text{Span}\{v_1, \dots, v_k\}^\perp$ is defined by

$$\text{Proj}(x, k) = x - \sum_{j=1}^k (v_j^* x) v_j \tag{11}$$

for normalized orthogonal family $\{v_1, \dots, v_k\}$, where v^* (row vector) is the transpose of v (column vector).

To study several eigenpairs, one may assume that the matrix A has real spectrum. Otherwise, for a complex eigenpair, one may have a conjugate one. This poses some difficulty.

At the last step, return to the original matrix:

$$\text{Eigenpair } (\lambda, g) \text{ of } A_1 \rightarrow \text{Eigenpair } (\lambda - \bar{\theta}, g) \text{ of } A. \tag{12}$$

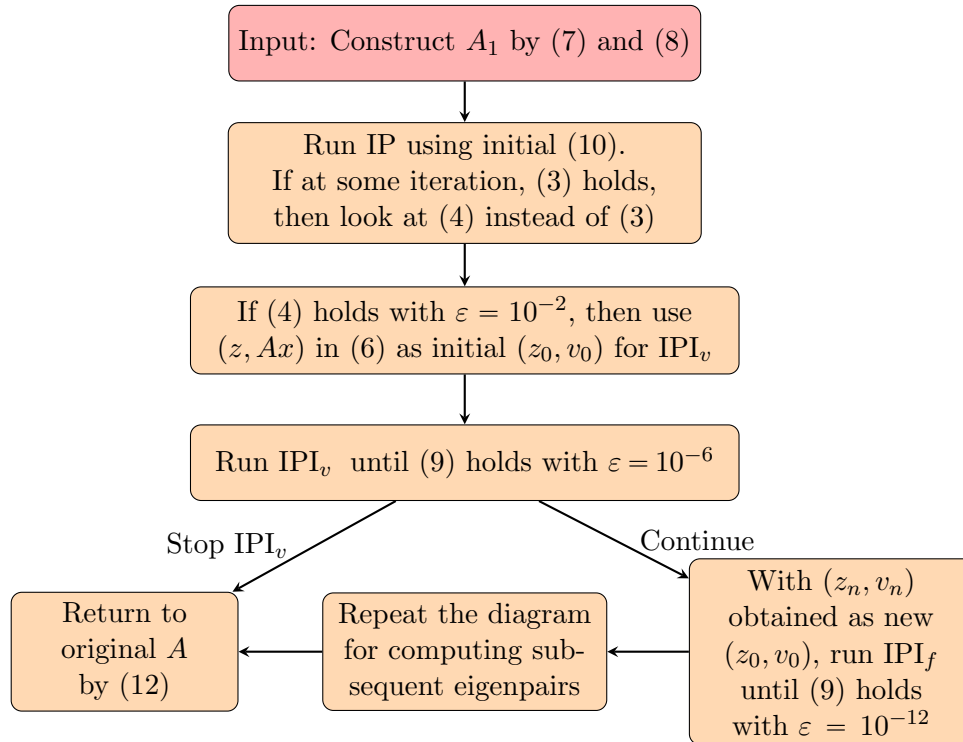


Figure 1: Flowchart of the preliminary version of the extended global algorithm

We now make some additional analysis on the preliminary version of the extended global algorithm in Fig. 1, as well as on the three algorithms used there: PI, IPI_v and IPI_f . While the localized estimation technique “check sign and locally bilateral estimates” (CS-LBE) mentioned above looks rather simple, the simplicity is precisely its biggest advantage – it can be applied to a rather wide range of applications, as we will see soon in the subsequent sections. The CS-LBE presents new opportunities to use techniques from a variety of fields such as optimization theory, machine learning, etc., since almost no theoretical results are available in this general setup. What we propose here is the (modified) PI. One may see a concrete example in the next section. Note that the choice of ε used for (4) or (9) in Fig. 1 may be changed according to different types of matrices used in various applications. Roughly speaking, one may use $\varepsilon \in [0.01, 0.1]$ instead of $\varepsilon = 0.01$ in (4) for medium size matrices. At this beginning step, we have used the main advantages of PI: it is safe and allows quite general initial vector, it has a good enough convergence and computing speed, except close too much to the target eigenvector.

Having the initial vector v_0 produced by the CS-LBE technique and the initial shift given by (7) at hand, we are ready to apply IPI_v to accelerate the computing speed. Under the conditions (3) and (4), instead of (5), we have

$$\min_{k \in \mathcal{N}_x} \frac{Ax}{x}(k) \leq \frac{x^*Ax}{x^*x} \leq \max_{k \in \mathcal{N}_x} \frac{Ax}{x}(k).$$

Replacing the term z given on the right-hand side by the middle one $\frac{x^*Ax}{\|x\|^2}$, the IPI_v becomes the so-called Rayleigh Quotient Iteration (abbrev. RQI), which is well-known a cubic algorithm (i.e., the iterative solutions generated by the algorithm converge cubically). Note that RQI is practical only if x is close enough to the target eigenvector, and hence is also a local algorithm. In particular, it is actually in a dangerous region once

$$\frac{x^*Ax}{x^*x} \in \left[\min_{k \in \mathcal{N}_x} \frac{Ax}{x}(k), \lambda \right).$$

However, since the precise local region over which the RQI is effective is not known, practical use of RQI often runs into the issue of converging to other eigenvectors that are close to the target ones. The last point is the main difference between our IPI_v and RQI. The proposed IPI_v ensures the algorithm robustness and allows convergence to the target eigenvector by adapting the shifts automatically. As verified by the practice in [4, 7] and the subsequent sections, the difference given in (4) goes to zero very fast. then so is the difference

$$\max_{k \in \mathcal{N}_x} \frac{Ax}{x}(k) - \frac{x^*Ax}{\|x\|^2}.$$

Hence, it is believable that IPI_v and RQI should have the same order of convergence speed, once RQI works.

For IPI_f , the initial vector v is similar to those of PI; the initial shift z of IPI_f should be bigger than the target λ . Otherwise, the algorithm becomes dangerous. Certainly, IPI_f is more effective if the initial pair (z, v) is closer to the target one. In Fig. 1, IPI_f is used in the last step to improve the target eigenvector. For which, IPI_v may no longer be practical since the inverse matrix would be degenerated too fast. The convergence by IPI_f can be faster than PI whenever the shift is close enough to the target λ from above.

We now summarize roughly the comparison the three algorithms: PI, IPI_v and IPI_f . Let

$\mathcal{D}(U)$ = Domain of suitable initial (vector, shift) of algorithm U ,

$s(U)$ = Convergence speed of algorithm U ,

$t(U)$ = Computational complexity of algorithm U .

From low to high is ordered by “<”.

Certainly, for PI, the shift variable is free in $\mathcal{D}(U)$. Then, roughly speaking, we have the following comparison

$$\begin{aligned}\mathcal{D}(\text{PI}) &\supset \mathcal{D}(\text{IPI}_f) \supset \mathcal{D}(\text{IPI}_v), \\ s(\text{PI}) &\leq s(\text{IPI}_f) \leq s(\text{IPI}_v), \\ t(\text{PI}) &< t(\text{IPI}_f) < t(\text{IPI}_v).\end{aligned}$$

A mixed algorithm of PI and IPI_v was used in [4, 7]. In the present paper, we introduce some extended algorithms which have more mixture of the above three algorithms, making best use of the advantage and bypassing the disadvantage of each of these three algorithms.

The next section is an exception where the algorithm is applied to the so-called Hermitizable complex matrix, not the real one treated in most part of the paper, to illustrate the wide use of the algorithm. Certainly, from the preliminary version to more general situation, additional work is required, as shown in §3 by the algorithm for large scale sparse matrix. The powerful algorithm is then illustrated by two examples in §4. If a reader is eager to take a look at the power of the proposed algorithm introduced in the paper, he or she can skip Sections 2, 3, and go directly to section 4.

2 Application to Hermitizable matrix

Consider the following complex matrix (cf. [5; Example 7])

$$A_0 = \begin{pmatrix} -6 & \frac{8}{5} - \frac{6i}{5} & \frac{8}{13} + \frac{14i}{13} & \frac{18}{17} + \frac{4i}{17} \\ 3 + \frac{9i}{4} & -\frac{55}{4} & -\frac{5}{13} + \frac{40i}{13} & \frac{30}{17} + \frac{35i}{17} \\ \frac{12}{5} - \frac{21i}{5} & -\frac{4}{5} - \frac{32i}{5} & -13 & \frac{60}{17} - \frac{66i}{17} \\ \frac{63}{10} - \frac{7i}{5} & \frac{28}{5} - \frac{98i}{15} & \frac{70}{13} + \frac{77i}{13} & -16 \end{pmatrix}.$$

A complex matrix $A = (a_{ij})$ is called Hermitizable if there exists a positive measure $\mu = (\mu_k)$ such that $\mu_i a_{ij} = \mu_j \bar{a}_{ji}$ for each pair (i, j) (due to [5]). It is called symmetrizable in the real context. It is easy to check that A_0 is Hermitizable with respect to μ :

$$\mu_0 = 1, \quad \mu_1 = \frac{8}{15}, \quad \mu_2 = \frac{10}{39}, \quad \mu_3 = \frac{20}{119}.$$

In general, from the proof of [5; Theorem 20], it is known that a complex matrix $A = (a_{ij})$ is Hermitizable w.r.t. measure $\mu = (\mu_k)$ iff

$$A = \text{Diag}(\mu)^{-1} A^H \text{Diag}(\mu) \quad [A^H := \bar{A}^*]. \tag{13}$$

Equivalently,

$$\hat{A} := \text{Diag}(\mu)^{1/2} A \text{Diag}(\mu)^{-1/2} \tag{14}$$

is Hermitian. Clearly, the transformation of the eigenpair (λ, g) of A to the one (λ, \hat{g}) of \hat{A} goes as follows.

$$(\lambda, g) \rightarrow (\lambda, \hat{g} = \text{Diag}(\mu)^{1/2} g). \tag{15}$$

At the moment,

$$\hat{A}_0 = \begin{pmatrix} -6 & (4 - 3i)\sqrt{\frac{3}{10}} & (4 + 7i)\sqrt{\frac{6}{65}} & (9 + 2i)\sqrt{\frac{7}{85}} \\ (4 + 3i)\sqrt{\frac{3}{10}} & -\frac{55}{4} & -\frac{2-16i}{\sqrt{13}} & (6 + 7i)\sqrt{\frac{14}{51}} \\ (4 - 7i)\sqrt{\frac{6}{65}} & -\frac{2+16i}{\sqrt{13}} & -13 & (10 - 11i)\sqrt{\frac{42}{221}} \\ (9 - 2i)\sqrt{\frac{7}{85}} & (6 - 7i)\sqrt{\frac{14}{51}} & (10 + 11i)\sqrt{\frac{42}{221}} & -16 \end{pmatrix}.$$

Due to (15), for computing the eigenpair of A_0 , it suffices to study the one for \hat{A}_0 . Hence, from now on, we need only to consider the matrix \hat{A}_0 .

The maximal eigenpair

We now start the algorithm given in Fig. 1. The computation in this section is done by using Mathematica (version 11.3) on PC.

Step 1. Construct A_1 . The upper bound produced by the first method given in §1 is $\theta(\hat{A}_0) = 29.957$. We now consider the second method.

Starting at $w_0 = \mathbf{1}/\|\mathbf{1}\|$ (cf. (10)) and use the following PI:

$$w_n = \hat{A}_0 v_{n-1}, \quad n \geq 1, \quad v_n := w_n / \|w_n\|, \quad n \geq 0.$$

Let

$$\begin{cases} \mathcal{N}(w) = \{k : |w(k)| > 0\}, \\ x_n = \left\{ \left| \frac{\hat{A}_0 w_n}{w_n} \right| (k), \quad k \in \mathcal{N}(w_n) \right\}, \\ y_n = \min_{k \in \mathcal{N}(w_n)} x_n(k), \quad z_n = \max_{k \in \mathcal{N}(w_n)} x_n(k). \end{cases}$$

Then in 5 iterations, the outputs are as follows.

$$\{z_n, y_n\}_{n=1}^5 : (21.2379, 5.26626), (27.0853, 17.7591), (27.2742, 17.6156),$$

$$(21.9304, 17.52740), (21.6953, 17.4757);$$

$$\{1 - y_n/z_n\}_{n=1}^5 : .752035, .344325, .354132, .200772, .194493.$$

Clearly, PI converges very well. Since z_4 and z_5 are closed each other, for them we have the same $\bar{\theta} = 22$ which is an upper bound of the spectral radius of \hat{A}_0 and is obviously smaller than the one obtained by the first method. Actually, if we continue PI for more iterations,

$$z_5 = 21.6953, z_{10} = 21.5148, z_{20} = 21.7481, z_{30} = 21.4567, z_{40} = 21.3927,$$

then we get the same $\bar{\theta}$, since the convergence becomes rather slow when z_n is close to the modulus of the maximal eigenvalue $\lambda^* = -21.3806$. Thus by (7), we have

$$A_1 = \hat{A}_0 + \bar{\theta} I$$

$$= \begin{pmatrix} 16 & (4 - 3i)\sqrt{\frac{3}{10}} & (4 + 7i)\sqrt{\frac{6}{65}} & (9 + 2i)\sqrt{\frac{7}{85}} \\ (4 + 3i)\sqrt{\frac{3}{10}} & \frac{33}{4} & -\frac{2-16i}{\sqrt{13}} & (6 + 7i)\sqrt{\frac{14}{51}} \\ (4 - 7i)\sqrt{\frac{6}{65}} & -\frac{2+16i}{\sqrt{13}} & 9 & (10 - 11i)\sqrt{\frac{42}{221}} \\ (9 - 2i)\sqrt{\frac{7}{85}} & (6 - 7i)\sqrt{\frac{14}{51}} & (10 + 11i)\sqrt{\frac{42}{221}} & 6 \end{pmatrix}.$$

To justify the effectiveness of the shift used here, let us compute the eigenvalues of A_1 :

$$21.8344, 12.5542, 4.24189, 0.619429.$$

It follows that there is only a little room (about 0.6) for the improvement of the shift $\bar{\theta} = 22$ to keep the positivity of the spectrum of A_1 . The transformation of the maximal eigenpair $(\lambda_1(A_1), g_1(A_1))$ of A_1 to the one $(\lambda_1, g_1) := (\lambda_1(A_0), g_1(A_0))$ of the original A_0 is as follows.

$$\lambda_1 = \lambda_1(A_1) - \bar{\theta}, \quad g_1 = \text{Diag}(\mu)^{-1/2} g_1(A_1). \tag{16}$$

Step 2. Run PI. As in Step 1, we use the following PI:

$$w_n = A_1 v_{n-1}, \quad n \geq 1, \quad v_n := w_n / \|w_n\|, \quad n \geq 0.$$

However, the original initial $\mathbb{1}/\|\mathbb{1}\|$ is replaced by $w_0 = (1 + i)\mathbb{1}/(\sqrt{2}\|\mathbb{1}\|)$. The reason is that for non-real A_1 , since the eigenvalues are all real, the eigenvectors should be non-real and so as a mimic, it is better to choose w_0 to be non-real. However, this is useless in Step 1, since a nonzero constant factor α can be ignored in the equation

$$|A(\alpha v)| = |\lambda| |\alpha v|.$$

We now come to the essential different point from the real case. Actually, for non-real A_1 , instead of the single equation (1), we have two:

$$\operatorname{Re}(A_1g) = \lambda \operatorname{Re}(g), \quad \operatorname{Im}(A_1g) = \lambda \operatorname{Im}(g).$$

Thus, it is naturally to split the original vector x (corresponding to g in the eigenequation) into two: x^R and x^I (corresponding to $\operatorname{Re} g$ and $\operatorname{Im} g$, respectively). Similarly we have \mathcal{N}_R and \mathcal{N}_I defined as follows.

$$\left\{ \begin{array}{l} \mathcal{N}_R(w) = \{k : |\operatorname{Re} w(k)| > 0\}, \quad \mathcal{N}_I(w) = \{k : |\operatorname{Im} w(k)| > 0\}; \\ p_n = A_1 w_n; \\ x_n^R = \left\{ \frac{\operatorname{Re} p_n}{\operatorname{Re} w_n}(k), k \in \mathcal{N}_R(w_n) \right\}, \quad x_n^I = \left\{ \frac{\operatorname{Im} p_n}{\operatorname{Im} w_n}(k), k \in \mathcal{N}_I(w_n) \right\}; \\ \text{weak} \left\{ \begin{array}{l} y_n = \left(\bigwedge_{k \in \mathcal{N}_R(w_n)} x_n^R(k) \right) \wedge \left(\bigwedge_{k \in \mathcal{N}_I(w_n)} x_n^I(k) \right), \\ z_n = \left(\bigvee_{k \in \mathcal{N}_R(w_n)} x_n^R(k) \right) \vee \left(\bigvee_{k \in \mathcal{N}_I(w_n)} x_n^I(k) \right); \end{array} \right. \\ \text{strong} \left\{ \begin{array}{l} y_n = \left(\bigwedge_{k \in \mathcal{N}_R(w_n)} x_n^R(k) \right) \vee \left(\bigwedge_{k \in \mathcal{N}_I(w_n)} x_n^I(k) \right), \\ z_n = \left(\bigvee_{k \in \mathcal{N}_R(w_n)} x_n^R(k) \right) \wedge \left(\bigvee_{k \in \mathcal{N}_I(w_n)} x_n^I(k) \right); \end{array} \right. \end{array} \right. \quad (17)$$

where $\alpha \wedge \beta = \min\{\alpha, \beta\}$ and $\alpha \vee \beta = \max\{\alpha, \beta\}$ for real α and β . The last two parts “weak” and “strong” need some explanation. First, the only difference is exchanging the “ \wedge ” and “ \vee ” in the middle of definition of (y_n, z_n) . To understand its essential difference, recall that condition (5) is now split into two:

$$\begin{aligned} (\operatorname{Re}_x) : \quad & \min_{k \in \mathcal{N}_R(x)} \frac{\operatorname{Re}(A_1x)}{\operatorname{Re} x}(k) \leq \lambda \leq \max_{k \in \mathcal{N}_R(x)} \frac{\operatorname{Re}(A_1x)}{\operatorname{Re} x}(k), \\ (\operatorname{Im}_x) : \quad & \min_{k \in \mathcal{N}_I(x)} \frac{\operatorname{Im}(A_1x)}{\operatorname{Im} x}(k) \leq \lambda \leq \max_{k \in \mathcal{N}_I(x)} \frac{\operatorname{Im}(A_1x)}{\operatorname{Im} x}(k). \end{aligned}$$

Now, for the “weak” case in (17) we simply adopt a weaker estimate of (y_n, z_n) from $(\operatorname{Re}_{x_n})$ and $(\operatorname{Im}_{x_n})$. And then the “strong” case should be clear. The weaker version of (y_n, z_n) plays the main role for the safety of converging to the required eigenpair, but makes a little slower convergence. While the stronger version makes a faster convergence but it requires that we are at the position close enough to the target eigenpair. Keeping these ideas in mind, one may adopt a mixture of these choices in designing the algorithms.

To fix the idea, throughout this section, the weak version of (y_n, z_n) is adopted at the first use of PI only in the computation of each eigenpair. For the other steps, we adopt the strong version.

It is the position to start the PI. In 6 iterations, the outputs are as follows.

$$\begin{aligned} \{z_n, y_n\}_{n=1}^6 : & (22.6771, -8.15858), (92.2205, 21.1287), (25.9135, 20.2681), \\ & (23.4485, 18.5274), (22.6331, 19.0585), (22.2652, 19.8867); \\ \{z_n - y_n\}_{n=1}^6 : & 30.8357, 71.0918, 5.64541, 4.92104, 3.57468, 2.37847; \\ \{1 - y_n/z_n\}_{n=1}^6 : & 1.35977, .770889, .217856, .209866, .15794, .106825. \end{aligned}$$

Note that here $y_1 < 0$. The outputs show that not only the components of $\operatorname{Re} w_n$ and $\operatorname{Re} w_{n-1}$ have the same sign once $n \geq 2$, but also the sequence of relative difference decreases quite quickly. We choose $n = 6$ ($\varepsilon \sim .1$) as the final iteration. Then, we have

$$v_6 = (.363237 + .491209 i, -.00786884 + .44046 i, .488441 - .0516616 i, \\ .326973 + .290776 i)^*.$$

Step 3. Run IPI_v . Starting at $(z_0, v_0) = (z_6, v_6)$ obtained in the last step, run IPI_v . Here we adopt a little different notation. Let w_n solve the equation

$$(z_{n-1}I - A_1)w_n = v_{n-1}, \quad n \geq 1.$$

and set $v_n = w_n/\|w_n\|$ again. Next, define $\mathcal{N}_R(w)$, $\mathcal{N}_I(w)$ and $\{x_n^R, x_n^I, y_n, z_n\}$ by (17) with the strong version of (y_n, z_n) .

Note that z_n and $1 - y_n/z_n$ are analogs of (6) and (4) in the complex context, respectively. Then, in 2 iterations, we obtain

$$(z_n, y_n)_{n=1}^2: (21.8358, 21.8324), (21.8344, 21.8344), \\ (z_n - y_n)_{n=1}^2: .00346973, 5.22045 \cdot 10^{-7}; \\ \{1 - y_n/z_n\}_{n=1}^2: .000158901, 2.39093 \cdot 10^{-8}, \\ v_2 = (.359825 + .494092 i, -.0061931 + .44037 i, .488017 - .054044 i, \\ .328093 + .289324 i)^*.$$

Moreover, $1 - y_2/z_2 \sim 10^{-8}$. This is not too small for the use of IPI_f in the next step.

Step 4. Run IPI_f . In the case we want to improve the above result furthermore, we adopt the IPI_f . Now, we take (z_2, v_2) from the last step as our new initial (z_0, v_0) . The only change to the last IPI_v is using the fixed $z_n \equiv z_0$. In 3 iterations, if we adopt the same precise digits as the last step, then we get the same outputs of (z_n, y_n) as the last one:

$$\{(z_n, y_n)\}_{n=1}^3: \text{the same pair } (21.8344, 21.8344); \\ \{y_n - z_n\}_{n=1}^3: \{10.6581, 0, 3.55271\} \cdot 10^{-15}; \\ \{1 - y_n/z_n\}_{n=1}^3: \{5.55112, 1.11022, 2.22045\} \cdot 10^{-16}. \\ v_3 = (.359825 + .494092 i, -.00619309 + .44037 i, .488017 - .054044 i, \\ .328093 + .289324 i)^*.$$

In what follows, we rewrite (z_3, v_3) as $(\lambda_1(A_1), g_1(A_1))$ which is regarded as the maximal eigenpair of A_1 .

The submaximal eigenpair

From the last part, we have obtained the maximal eigenpair $(\lambda_1(A_1), g_1(A_1))$, at the machine level of precision, as follows.

$$\begin{aligned}\lambda_1(A_1) &= 21.834441785286337, \\ g_1(A_1) &= (.35982503686976175 + .49409186313969483 i, \\ &\quad - .006193088194633169 + .44037016603620777 i, \\ &\quad .48801737987976945 - .054043998846425696 i, \\ &\quad .3280927162424674 + .28932402046371486 i)^*.\end{aligned}$$

Step 1. Run modified PI. As an analog (11), the projection of the vector w on the space $\text{Span}(g_1(A_1))^\perp$ is as follows.

$$w - \frac{g_1(A_1)^H w}{(g_1(A_1))^H g_1(A_1)} g_1(A_1) \quad [g^H := \bar{g}^*].$$

The modified PI means the use of the usual PI with the modification by the projection above at each step. That is

$$\begin{aligned}w_0 &= \frac{(1+i)\mathbf{1}}{\sqrt{2}\|\mathbf{1}\|}, \\ u_n &= w_n - \frac{g_1(A_1)^H w_n}{(g_1(A_1))^H g_1(A_1)} g_1(A_1), \quad n \geq 0, \\ w_n &= A_1 \frac{u_{n-1}}{\sqrt{u_{n-1}^H u_{n-1}}}, \quad n \geq 1.\end{aligned}$$

Next, similar to (17), replacing w and w_n by u and u_n respectively, we can define \mathcal{N}_R , \mathcal{N}_I , p_n , x_n^R , x_n^I , and the weak version of (y_n, z_n) . Starting at w_0 and running the modified PI, in 5 iterations, we obtain

$$\begin{aligned}\{(z_n, y_n)\}_{n=1}^5 &: (13.3067, 1.07981), (12.7854, -32.9231), (18.4212, 10.2147), \\ &\quad (13.9055, 11.5768), (12.9665, 12.1958); \\ \{z_n - y_n\}_{n=1}^5 &: 12.2269, 45.7085, 8.20655, 2.32871, .770683; \\ \{1 - y_n/z_n\}_{n=1}^5 &: .918852, 3.57505, .445495, .167467, .0594367.\end{aligned}$$

Note that here $y_2 < 0$. We stop at $n = 5$ since $1 - y_5/z_5$ is small enough, even though it is bigger than 10^{-2} . Then, we have

$$\begin{aligned}z_5 &= 12.9665, \\ v_5 &= (.0677311 - .786181 i, - .190409 + .21529 i, .356539 + .247925 i, \\ &\quad .0428153 + .322965 i)^*.\end{aligned}$$

Step 2. Run IPI_v. Taking (z_5, v_5) from the last step as new (z_0, v_0) , run IPI_v. Let w_n solve the equation

$$(z_{n-1}I - A_1)w_n = v_{n-1}, \quad n \geq 1,$$

and define first $v_n = w_n/\|w_n\|$, and then $\mathcal{N}_R(w)$, $\mathcal{N}_I(w)$ and $\{x_n^R, x_n^I, y_n, z_n\}$ by (17) with the strong version of (y_n, z_n) . Now, in 3 iterations, we obtain

$$\begin{aligned} \{(z_n, y_n)\}_{n=1}^3 &: (12.5546, 12.5507), (12.5542, 12.5542), (12.5542, 12.5542); \\ \{z_n - y_n\}_{n=1}^3 &: .00385406, 1.50454 \cdot 10^{-7}, 3.55271 \cdot 10^{-15}; \\ \{1 - y_n/z_n\}_{n=1}^3 &: .000306985, 1.19843 \cdot 10^{-8}, 3.33067 \cdot 10^{-16}. \\ v_2 &= (.604525 - .508517i, -.301145 + .0168374i, .0761289 + .417867i, \\ &\quad -.196423 + .2569i)^*. \\ v_3 &= (.604525 - .508517i, -.301145 + .0168374i, .0761289 + .417867i, \\ &\quad -.196423 + .2569i)^*. \end{aligned}$$

In the case we do not want to go further, we can stop here at $n = 3$ since $1 - y_3/z_3 \sim 10^{-16}$ is sufficiently small. It is actually too smaller to go to the next step, otherwise it would cost some computational error.

Step 3. Run IPI_f. To have a test, setting (z_0, v_0) to be (z_2, v_2) obtained in the last step, run IPI_f also in 3 iterations, we obtain the same output $z_n = y_n = 12.5542$ for $n = 1, 2, 3$, and

$$\begin{aligned} \{z_n - y_n\}_{n=1}^3 &: \{3.55271, 3.55271, 8.88178\} \cdot 10^{-15}; \\ \{1 - y_n/z_n\}_{n=1}^3 &: \{3.33067, 3.33067, 6.66134\} \cdot 10^{-16}. \end{aligned}$$

Moreover

$$\begin{aligned} v_3 &= (.6045251632662887 - .5085174051419706i, \\ &\quad -.3011448284487476 + .016837350902488956i, \\ &\quad .07612884589652998 + .4178669662768421i, \\ &\quad -.19642273529356236 + .2568995483366027i)^*. \end{aligned}$$

The present v_3 has a much higher precise level than v_2 obtained in Step 2. We now regard (z_3, v_3) as the submaximal eigenpair $(\lambda_2(A_1), g_2(A_1))$ of A_1 .

Similarly, one can compute the other eigenpairs of A_1 but we are not going to the details here.

Finally, we return to the original eigenpairs of A_0 by (16):

$$\begin{aligned} \lambda_1 &= \lambda_1(A_1) - 22 = -.165558, \\ g_1 &= \text{Diag}(\mu)^{-1/2} g_1(A_1) = (.359825 + .494092i, -.00848024 + .603002i, \\ &\quad .963757 - .106728i, .800304 + .705737i)^* \\ \lambda_2 &= \lambda_2(A_1) - 22 = -9.44576, \\ g_2 &= \text{Diag}(\mu)^{-1/2} g_2(A_1) = (.604525 - .508517i, -.41236 + .0230555i, \\ &\quad .150342 + .825221i, -.479127 + .626645i)^* \end{aligned}$$

It is nice chance to learn some thing from the above computation.

1) In the earlier papers [3] and [7], the sequence $\{z_n\}$ should control the maximal eigenvalue from above, due to the Perron-Frobenius theorem and the C-W formula mentioned in §1. However, this may not be true in the present general setup, as can be seen from Step 1 of computing the maximal eigenpair,

$$z_1 < |\lambda^*(\hat{A}_0)| = 21.3806 < z_2 < z_3 > z_4 > z_5 > |\lambda^*(\hat{A}_0)|,$$

the sequence $\{z_n\}$ arrives its maximum at z_3 . In Step 2, we have similarly,

$$\lambda_1(A_1) = 21.8344 < z_1 < z_2 > z_3 > \cdots > z_6 > \lambda_1(A_1).$$

In this case, it follows that the sequence $\{z_n\}$ arrives its maximum at z_2 , and then it goes down. In both cases, the sequence $\{1 - y_n/z_n\}$ is decreasing in n quickly.

Step 1 in computing the submaximal eigenpair is much more interesting. It illustrates the unstable property of $\{z_n\}$ at the beginning. Here we adopt the modified PI. We have

$$z_1 > z_2 > \lambda_2(A_1) = 12.5542 < z_3 > z_4 > z_5 > \lambda_2(A_1).$$

Correspondingly, for $\xi_n := 1 - y_n/z_n$, we have

$$\{\xi_n\}_{n=1}^5: .918852, 3.57505, .445495, .167467, .0594367.$$

A big jump happens at z_3 since as mentioned earlier, $y_2 < 0$ and so the check sign (CS) is necessary. At $n = 5$, even though $\xi_5 \sim .059 > .01$, but $z_5 = 13.0168 > \lambda_2(A_1)$, and so the use of IPI_v in the subsequent step is safe. Roughly speaking, one can stop PI at the m th iteration, if starting from z_m , the sequence $\{z_n\}_{n \geq m}$ converges decreasingly. It is the case if the matrix has nonnegative off-diagonals, as studied in [3, 7], or the examples given in §4. In view of this point, one may reduce the number of iterations in using PI at the beginning of the computation for the maximal/submaximal eigenpair. More precisely, the PI (*Step 2*) for computing the maximal eigenpair needs only $6 - 2$ iterations and for submaximal one, it requires only $5 - 1$ iterations. For subsequent IPI_v or IPI_f , the number of iterations remains the same as the original in the both cases.

2) All the computations above show that the sequence $\{1 - y_n/z_n\}_n$, may be except a few of terms at the beginning, is monotone decreasing and converges, much stable than the other sequences, $\{z_n\}$ or $\{|1 - z_n/z_{n-1}|\}$, in the present general setup. Among the computations above, the exceptional part of the sequence $\{\xi_n = 1 - y_n/z_n\}$ appears mainly in the last case just discussed above. For which, the first 2 terms are unstable, especially the second one is bigger than 1 since $y_2 < 0$ as mentioned before. The stability starts at the third term. It follows that the use of the sequence $\{1 - y_n/z_n\}$ is more practical and is actually adopted in the preliminary version of the algorithm given in Fig. 1. For this reason, it seems more precise to rename the “CS-LBE” technique

by adding the relative difference (RD): CS-RD-LBE technique in the general situation.

It is hoped that the algorithm given here could be used in the quantum mechanics computation (cf. [6]).

For the remainder of the paper, we return to real matrices for which Hermitizable becomes symmetrizable. By (15), we can reduce a symmetrizable matrix to a symmetric one. Then, by using (16), we can assume that the given symmetric matrix has a nonnegative spectrum.

3 A version of the global algorithm for large scale matrices

As remarked at the end of the last section, we need only to study the symmetric matrix having nonnegative eigenvalues. In this section, we describe the extended global (or global for short) algorithm for computing the top eigenpairs of a large sparse matrix. This algorithm computes the eigenpairs sequentially, starting from the top eigenpair and then uses the previously computed $(i - 1)$ eigenpairs to compute the next i th eigenpair. The flowchart of the algorithm for computing the i th eigenpair is shown in Fig. 2.

We first summarize the key points of the proposed algorithm as follows.

- The inputs to the algorithm are the first $i - 1$ eigenpairs $\{(\lambda_j, v_j), j = 1, \dots, i - 1\}$ that have already been computed using the same algorithm. Here, λ_j denotes the j th largest eigenvalue and v_j denotes the j th eigenvector.
- At the initial iteration $n = 0$, we initialize with y_0 given by (10).
- Starting from the initial vector y_0 , run a procedure called “Check sign with locally bilateral estimates (CS-LBE)” to determine initial shift z_0 and the corresponding eigenvector estimate x_0 . This procedure involves running multiple power iterations with projection and check sign, and estimating z_0 based on the locally bilateral estimates (an analog of (5)). Details of the CS-LBE procedure will be described later.
- Given x_n and z_n , determined by the CS-LBE procedure, we then perform one iteration of the IPI_v: $(z_n I - A)y_n = x_n$ to solve for the updated eigenvector estimate y_n .
- Given y_n , we will run the CS-LBE procedure to determine the next shift z_{n+1} and the corresponding eigenvector estimate x_{n+1} .
- Given x_{n+1} , we will check whether the accuracy of x_{n+1} has improved compared to that of earlier iterations. Detailed criterion used to evaluate the accuracy of the eigenvector (which corresponds to the amplitude of LBE given in §1) will be described later.
- If the accuracy of x_{n+1} has not improved compared to earlier iterations, then the algorithm has converged. It then outputs the i th eigenpair

- $\lambda_i = z_{n+1}$, $v_i = x_{n+1}$ and proceeds with the computation of the $(i+1)$ th eigenpair. On the other hand, if the accuracy of x_{n+1} has improved compared to earlier iterations, then the algorithm proceeds with the next iteration of IPI_v .
- Note that for the n th iteration of the IPI_v , if the condition $|z_n - z_{n-1}| < 10^{-8}$ is met, then we stop updating the shift and set $z_n = z_{n-1}$ instead. That is, we turn to IPI_f .

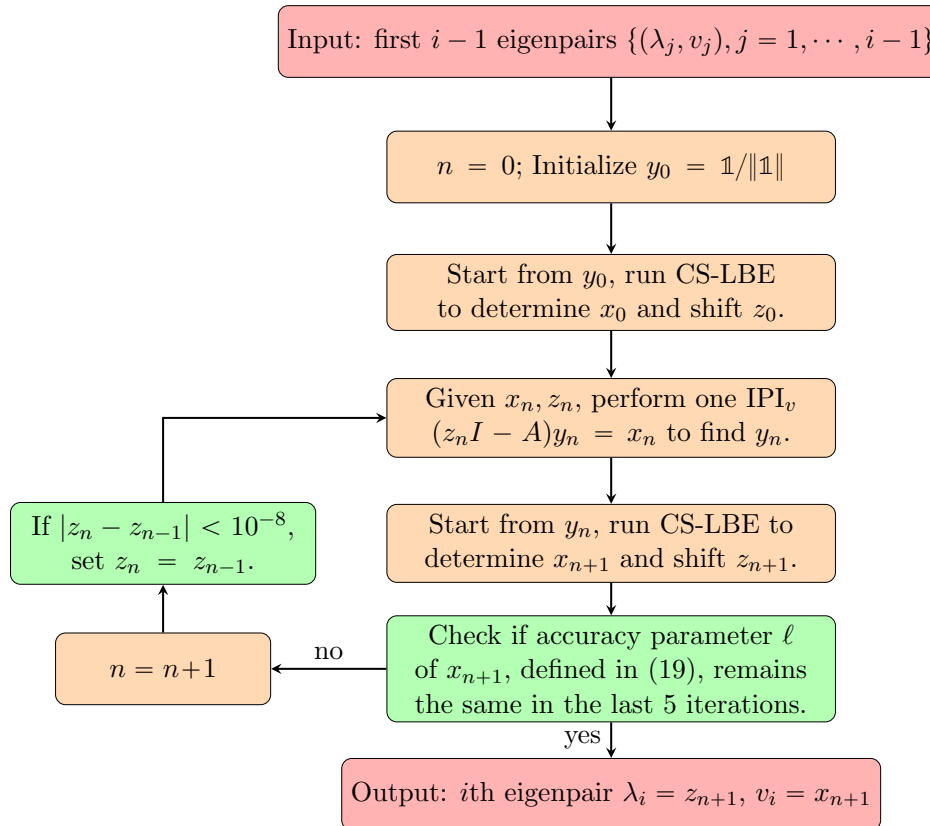


Figure 2: Flowchart of the main algorithm for computing the i th eigenpair. Assume that the previous $i - 1$ eigenpairs have been computed.

Next, we provide more details of the global algorithm. We will first define the CS-LBE procedure. This procedure requires the following two basic operations.

Projection operator This is defined by (11). It ensures that after projection, the vector $\text{Proj}(x, k)$ is orthogonal to the linear space $\text{Span}(\{v_j, j = 1, \dots, k\})$.

Shift Evaluation Given a current estimate of the eigenvector x , we aim to determine a proper shift based on the locally bilateral estimates. For large

sparse matrices, the components of x may decay to zero very quickly. Thus, estimation of the shift using all components of x can be unreliable, and sensitive to the estimation errors of those components of x with very small amplitudes. In our algorithm, we propose to calculate the shift based on only the principal components of x such that $|x(i)| \geq t(x)$, where $t(x)$ is a threshold value to be determined. Estimating the shift based on only principal components with larger amplitude improves the estimate of the shift. Let x be a unit vector in the L_2 -space of dimension N . Given x , we define the shift evaluation function, denoted by $z(x)$, as follows. Let x_a denote the sorted vector of $|x|$ in the descending order. Let n' be the smallest integer such that $\sum_{i=1}^{n'} x_a(i)^2 \geq \epsilon_0$. Typically, we set $\epsilon_0 = 0.9$. This means that the first n' components of vector x_a captures 90% of the energy of vector x . Let $t(x) = |x_a(n')|$. Given x and $y = Ax$, we define the shift evaluation function $z(x)$ by considering only the major components of x such that $|x(i)| \geq t(x)$:

$$z(x) = \max_{\{i:|x(i)|\geq t(x)\}} \frac{y}{x}(i) \quad \left[\frac{y}{x}(i) := \frac{y(i)}{x(i)} \right]. \tag{18}$$

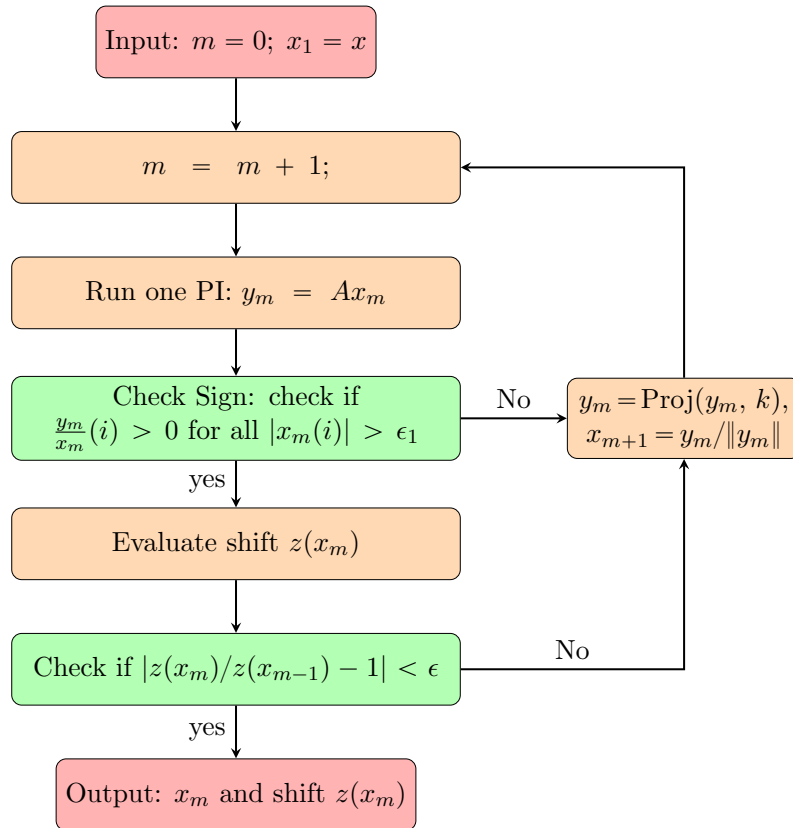


Figure 3: Flowchart of the compute-shift with locally bilateral estimates (CS-LBE) procedure.

This is a modification of (6) for the large scale matrix. Note that in (18), we adaptively determine the principal components of the estimated eigenvector x over iterations. This is important to obtain good estimates of the shift $z(x)$.

In Fig. 3, we show the flow-diagram of the CS-LBE procedure in using the *modified PI* (cf. Step 1 of computing the submaximal eigenpair given in §2). The input to this procedure is an initial estimate of the eigenvector x . The subscript m is the index of the PI. At the m th PI, we calculate $y_m = Ax_m$. This is followed by a check sign step in which we check whether the condition that

$$\frac{y_m}{x_m}(i) > 0 \text{ is satisfied for all } |x_m(i)| > \epsilon_1 \quad (\text{analog of (3)}).$$

If check sign fails, then we conduct a projection step on y_m to make sure that the resulting vector is orthogonal to the linear space generated by the first $k - 1$ eigenvectors. Then we set $x_{m+1} = y_m / \|y_m\|$ and then proceeds to the next PI. If the check sign is successful, then we compute the shift $z(x_m)$ in the next step. The shift evaluation function z is defined as in (18). We will compare the newly computed shift $z(x_m)$ with the previous shift $z(x_{m-1})$ to see whether the shift values have converged. If so, we will finish the procedure and output the updated estimate of the eigenvector x_m and the shift $z(x_m)$. Otherwise, the algorithm will proceed with the next PI.

Check eigenvector accuracy Most works in the literature use L_2 norm of the error vector between the true eigenvector and the estimated eigenvector to evaluate the accuracy of the eigenvector estimation. However, since L_2 norm is obtained by summing over all components of the error vector, it can not accurately describe the accuracy of the individual components. In this work, we adopt a different metric by examining the accuracy of component-wise ratios of $y = Ax$ and x . By the definition of the eigenvector, for each component $x(k) \neq 0$, then the ratio $y(k)x(k)^{-1}$ should equal the eigenvalue λ . This is a challenging task for the setting of large matrices due to the high matrix dimension and the rapid decay of the eigenvectors. Typically, when the amplitude of a component $x(k)$ is large, the estimation tends to be more accurate, and thus the ratio $y(k)x(k)^{-1}$ will be closer to the eigenvalue λ . For small $x(k)$, the ratio $y(k)x(k)^{-1}$ tends to deviate away from λ due to estimation inaccuracy. Hence, it is meaningful to consider the amplitude range of $x(k)$ over which all $y(k)x(k)^{-1}$ are close to λ .

We now arrive at the second localized estimation technique: *Accuracy of the principal components of the approximating eigenvector*.

Consider an estimated eigenvector x of dimension N . Let I denote a permutation of $\{1, 2, \dots, N\}$ obtained by sorting the components of $|x|$ in the descending order. Given I , we define \tilde{x} as $\tilde{x}(i) = x(I(i))$, $i = 1, \dots, N$. Given the same I , we let $y = Ax$ and define \tilde{y} as $\tilde{y}(i) = y(I(i))$, $i = 1, \dots, N$.

- Let $m' = \max_i \{i : |\tilde{x}(i)| > 0\}$.

- The accuracy parameter ℓ of the estimated eigenvector specifies the number of reliable components of \tilde{x} . It is defined as

$$\ell = \max_{1 \leq i \leq m'} \left\{ i : \max_{1 \leq j \leq i} \frac{\tilde{y}(j)}{\tilde{x}(j)} - \min_{1 \leq j \leq i} \frac{\tilde{y}(j)}{\tilde{x}(j)} < 10^{-6} \right\}. \quad (19)$$

- Based on the definition of ℓ in (19), we see that the estimated eigenvector x achieves a high accuracy for the largest ℓ components (in absolute value). In other words, the components of x have high accuracy for all components $x(i)$ such that $|x(i)| \geq |\tilde{x}(\ell)|$.

Note that in the proposed algorithm shown in Fig. 2, we calculate the accuracy parameter ℓ for the estimated eigenvector x_{n+1} according to 19. As the algorithm proceeds, ℓ will increase over iterations. We terminate the algorithm if ℓ no longer increases over five consecutive iterations.

4 Application to large scale sparse matrices

In this section, we provide two examples of using the global algorithm to compute the top 6 eigenpairs. The two large matrices come from the SuiteSparse Matrix Collection, publicly available at <https://sparse.tamu.edu>. We will compare the proposed algorithm with two other methods. One is the Matlab Eigs function, which computes the top six eigenpairs of large, sparse matrices. The other is the modified power iteration method, where we perform the standard power iteration together with the projection step to compute the top six eigenpairs. All the experiments presented in this section are executed on an AMD Ryzen 5 2600 Six-Core Processor with single core CPU speed 3.85 GHz, Memory 32 GB. Matlab version is R2015b Windows 10. Related work on computing the top eigenpair for large sparse matrices include [12], [11], [8]. In particular, [12], [11] consider the use of inverse iterations using fixed shifts. This work differs from [12], [11] in the use of the proposed (CS-LBE) procedure to adaptively compute the shifts. Furthermore, the estimated eigenvector accuracy considered in [12], [11], [8] (for the largest eigenpair only) is similar to that of the Matlab Eigs function, which only guarantees the accuracy of a small number of large principal components. In comparison, the proposed global algorithm achieves a high accuracy for even eigenvector components with an exceedingly small magnitude.

dixmaanl dataset

This matrix has a dimension of $N = 60000$. *The number of nonzero elements* (abbrev. *nz*) is 299998, This matrix is nonnegative, symmetric, and the range of the elements is between 0 and 154.8089. The sparsity pattern of this matrix is shown in Fig. 4(a).

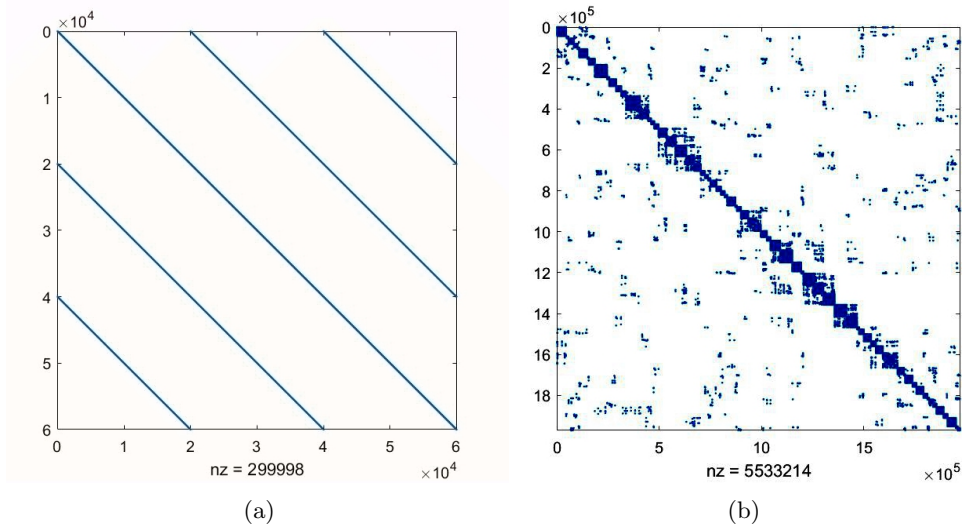


Figure 4: Sparsity of the two datasets. (a) dixmaanl (b) roadNet-CA

Table 1: dixmaanl dataset. Computed top 6 eigenvalues using the Global algorithm, eigs, and modified PI.

	global	eigs	PI
λ_1	317.0152899359881	317.0152899359666	317.0152899359881
λ_2	317.0058090659085	317.0058090659162	317.0058090659074
λ_3	316.9980633932568	316.9980633932683	316.9980633932562
λ_4	316.9912300516546	316.9912300516576	316.9912300516548
λ_5	316.9849936226963	316.9849936226929	316.9849936226971
λ_6	316.9791911040992	316.9791911040974	316.9791911040990

In Table 1, we show the estimated top 6 eigenvalues obtained by each method. We see that all three methods provide similar eigenvalue estimates that agree with each other up to 10 decimal points.

In Table 2, we provide detailed comparisons of the three methods in terms of the accuracy of the eigenvector, the complexity, and the running time. Each row corresponds to results associated with the i th eigenpair. For instance, the row corresponds to λ_1 reads as follows. The global algorithm estimates the largest (in magnitude) $\ell = 56515$ components of the eigenvector v_1 accurately (see (19)). This represents accurate estimation of all components of v_1 with a magnitude that is greater or equal to $|v_1(\ell)| = 8.1 \cdot 10^{-316}$. The triple (288, 40, 5) means that in order to achieve this accuracy, the global algorithm took a total of 288 power iterations, including 40 iterations for inverse power iterations (35 of IPI_f and 5 of IPI_v). The global algorithm took 5.1 seconds to compute the first eigenpair while achieving this high level of accuracy. In

Table 2: dixmaanl dataset. Results and complexity using the Global algorithm, eigs, and modified PI.

	Global				eigs		
	ℓ	$ \tilde{x}(\ell) $	# iteration	time	ℓ	$ \tilde{x}(\ell) $	time
1st	56515	8.1e-316	(288, 40, 5)	5.1	3311	3.7e-08	30
2nd	57294	8.7e-316	(319, 45, 6)	5.8	3883	3.2e-08	
3rd	57936	9.2e-316	(244, 40, 5)	4.6	4306	4.1e-08	
4th	58515	8.7e-316	(274, 45, 7)	5.2	4599	8.6e-08	
5th	59020	1.2e-315	(276, 45, 5)	5.4	5138	2.9e-08	
6th	59536	9.1e-316	(312, 45, 6)	6.3	5401	5.2e-08	

	Modified PI			
	ℓ	$ \tilde{x}(\ell) $	time	# PI
1st	56460	1.9e-315	894	1.5e+06
2nd	57246	1.8e-315	1173	1.5e+06
3rd	57896	1.7e-315	1442	1.5e+06
4th	58472	1.7e-315	1718	1.5e+06
5th	58988	2.0e-315	1998	1.5e+06
6th	59480	2.0e-315	2292	1.5e+06

comparison, the Matlab eigs function, which computes all 6 top eigenpairs all at once, has a much inferior eigenvector accuracy. Only the largest $\ell = 3311$ components of estimated v_1 achieve the desired accuracy of (19) and these components are at least $|v_1(\ell)| = 3.7 \cdot 10^{-8}$ in magnitude. The total computation time of the eigs function for all 6 eigenpairs is 30 seconds. This is comparable with the total computation time of the global algorithm, however, with a significantly lower level of eigenvector accuracy. For the modified PI, we see that it can achieve an accuracy that is comparable to that of the global algorithm. However, the computation time is significantly longer. Due to its slow convergence, it takes 894 seconds and a total of $1.5 \cdot 10^6$ PIs in order to attain a similar accuracy as that of the global algorithm. Similar observations are made for the estimations of the other 5 eigenpairs. The proposed global algorithm achieves the best accuracy with the shortest computation time. We note that the main difference between the Global algorithm and the modified PI is that the former uses inverse power iteration with adaptive shifts, whereas the latter uses standard power iterations. Our results shown that the proposed CS-LBE procedure for computing the variable shifts is crucial in accelerating the convergence speed of the algorithm.

In Table 3, for each eigenpair, we show the value of the shifts used in the Global algorithm. The shifts are generated using the CS-LBE procedure. For instance, the column labeled as “1st” lists 5 values of the shifts z_i , $i = 1, \dots, 5$,

used in the estimation of the 1st eigenpair. We see that z_i approaches the true λ value (shown in the last row) quickly. For the first eigenpair, only 5 different shifts are needed. In comparison, for the 4th and the 6th eigenpair, more shifts 7, and 6, respectively, are needed.

Table 3: dixmaanl dataset. Shifts used by the Global algorithm.

	1st	2nd	3rd
z_1	317.2018759831095	317.0149029206981	317.0054220600994
z_2	317.0220587013249	317.0412999365110	317.0056140237707
z_3	317.0165531440067	317.0183499796456	316.9974443732343
z_4	317.0152788610227	317.0044840756761	316.9980602821128
z_5	317.0152899359775	317.0057627487807	316.9980633932562
z_6		317.0058090643057	
λ	317.0152899359881	317.0058090659085	316.9980633932568
	4th	5th	6th
z_1	316.9976763951934	316.9908430604246	316.9846066377027
z_2	317.0174070334262	316.9924907259373	317.0002253316557
z_3	316.9879937432648	316.9843539028472	316.9767242599030
z_4	316.9896903234464	316.9849885385036	316.9784124921462
z_5	316.9910317369073	316.9849936226933	316.9791679223474
z_6	316.9912298325970		316.9791911036812
z_7	316.9912300516546		
λ	316.9912300516546	316.9849936226963	316.9791911040992

roadNet-CA dataset

For this dataset, the dimension of the matrix is $N = 1971281$. This matrix corresponds to a graph of the road network of California. Each element is either 0 or 1. The sparsity pattern of this matrix is shown in Fig. 4(b). The number of nonzero elements in the matrix is $\text{nz} = 5533214$, see Fig. 4(b). In Table 4, we show detailed comparisons of the three methods in terms of the accuracy of the eigenvector, the complexity, and the running time. We see that the Global algorithm reaches very good accuracy in terms of ℓ and $|\tilde{x}(\ell)|$ for all 6 eigenpairs. Due to the increased matrix dimension, the computation time increases compared to that of the dixmaanl dataset. The eigs function can compute the top 6 eigenpairs quickly, using only a total of 38 seconds, but with a much inferior accuracy in ℓ and $|\tilde{x}(\ell)|$. The modified PI algorithm can achieve a very good accuracy for the top 3 eigenpairs, despite a longer computation time for using a high number of PI. The accuracy of the remaining 3 eigenpairs is much worse for the given number of PI.

Table 4: roadNet-CA dataset. Results and complexity using the Global algorithm, eigs, and modified PI.

	Global				eigs		
	ℓ	$ \tilde{x}(\ell) $	# iterations	time	ℓ	$ \tilde{x}(\ell) $	time
1st	1933344	2.8e-317	(244, 35, 3)	309	1543	8.7e-10	38
2nd	1926704	3.0e-317	(245, 35, 3)	322	1413	1.1e-09	
3rd	1957027	2.8e-295	(226, 30, 3)	276	2004	1.0e-09	
4th	1948213	2.2e-317	(243, 30, 3)	285	2190	5.3e-10	
5th	1956156	2.3e-317	(242, 30, 3)	293	2409	2.9e-10	
6th	1923583	2.7e-317	(282, 30, 2)	296	1648	7.8e-10	

	Modified PI			
	ℓ	$ \tilde{x}(\ell) $	# PI	time
1st	1933452	2.0e-317	1.0e+04	381
2nd	1926900	2.0e-317	2.5e+04	1432
3rd	1957027	2.8e-295	2.7e+04	2062
4th	49653	1.6e-33	5e+04	4700
5th	62901	1.8e-33	7e+03	776
6th	1923767	1.9e-317	5.0e+04	6671

Table 5: roadNet-CA dataset. Computed top 6 eigenvalues using the Global algorithm, eigs, and modified PI.

	global	eigs	PI
λ_1	4.638361867351406	4.638361867351387	4.638361867351406
λ_2	4.527027931848926	4.527027931848909	4.527027931848924
λ_3	4.451588326941737	4.451588326941750	4.451588326941737
λ_4	4.390275021532836	4.390275021532792	4.390275021532837
λ_5	4.383736144475813	4.383736144475774	4.383736144475815
λ_6	4.325729176980614	4.325729176980572	4.325729176980615

In Table 5, we show the estimated top 6 eigenvalues using the three algorithms. They all find similar eigenvalues.

In Table 6, we show the shifts produced by the CS-LBE procedure. We observe that, despite the higher dimension of this dataset, the shift values converge to the eigenvalues quickly. Up to 3 shift values are sufficient to approach the eigenvalues.

Acknowledgments The first author thanks Professors Jia, Z.G. and Pang, H.K. and their teams for the fruitful discussions, verifying and suggestions which improve the quality of the paper. The teams are now continuously working on applications of the proposed method, such as computing the sparse principal components of medical

Table 6: roadNet-CA dataset. Shifts used by the Global algorithm.

	1st	2nd	3rd
z_1	4.651095152690492	4.541091827266276	4.457490006778257
z_2	4.638369301398686	4.527034278350056	4.451618990253862
z_3	4.638361867350882	4.527027931841913	4.451588326915770
λ	4.638361867351406	4.527027931848926	4.451588326941737
	4th	5th	6th
z_1	4.390768119815626	4.384210430746412	4.325729209088518
z_2	4.390275047542154	4.383736186751131	4.325729176980588
z_3	4.390275021532815	4.383736144475802	
λ	4.390275021532836	4.383736144475813	4.325729176980614

images and others. Special thanks to Professor Xie, Y.C. for his support and great help during the period the author worked at the university. Research supported in part by National Natural Science Foundation of China (Grant Nos. 12090011, 11771046), National Key R & D Program of China (No. 2020YFA0712900), the project from the Ministry of Education in China, and the Project Funded by the Priority Academic Program Development of Jiangsu Higher Education Institutions.

References

- [1] Chen, M.F. (2005). *Eigenvalues, Inequalities, and Ergodic Theory*. London: Springer.
- [2] Chen, M.F. (2016). *Efficient initials for computing maximal eigenpair*. Front. Math. China 11(6): 1379–1418.
- [3] Chen, M.F. (2017a). *Global algorithms for maximal eigenpair*. Front Math China 12(5): 1023–1043.
- [4] Chen, M.F. (2017b). *Trilogy on computing maximal eigenpair*. In: Yue, W., Li, Q. L., Jin, S., Ma, Z., eds. “Queueing Theory and Network Applications”. QTNA 2017. Lecture Notes in Comput. Sci., Vol. 10591. Cham: Springer, 312–329.
- [5] Chen, M.F. (2018). *Hermitizable, isospectral complex matrices or differential operators*. Front Math China 13(6): 1267–1311.
- [6] Chen, M.F., Jia, Z.G. and Pang, H.K. (2021). *Computing top eigenpairs of Hermitizable matrix*. Front. Math. China 16(2): 345–379.
- [7] Chen, M.F., Li, Y.S. (2019). *Improved global algorithms for maximal eigenpair*. Front. Math. China 14(6): 1077–1116.
- [8] Lei, Q., Zhong, K., Dhillon, I.S. (2016). *Coordinate-wise Power Method*. Proc. Advances in Neural Information Processing Systems, 2056–2064.
- [9] Press, W.H. et al. (2007). *Numerical Recipes—The Art of Scientific Computing*, 3rd ed. Cambridge Univ. Press.
- [10] Varga, R.S. (2004). *Geršgorin and His Circles*. Springer.
- [11] Wang, J.L., Wang, W.R., Garber, D., Srebro, N. (2018). *Efficient coordinate-wise leading eigenvector computation*. Proc. Algorithmic Learning Theory, PMLR, 806–820.

- [12] Xu, Z.Q. (2018). *Gradient descent meets shift-and-invert preconditioning for eigenvector computation*. Proc. Advances in Neural Information Processing Systems, 31: 2825–2834.

Hermitizable, Isospectral Matrices or Differential Operators

Mu-Fa Chen

(Jiangsu Normal University and Beijing Normal University)

September 4, 2021

Abstract

This paper reports the study on Hermitizable problem for complex matrix or second order differential operator. That is the existence and construction of a positive measure such that the operator becomes Hermitian on the space of complex square-integrable functions with respect to the measure. In which case, the spectrum are real, and the corresponding isospectral matrix/differential operators are described. The problems have a deep connection to computational mathematics, stochastics, and quantum mechanics.

According to the different objects: matrix and differential operator, the report is divided into two sections, with emphasis on the first one.

1 Hermitizable, isospectral matrices

Let us start at the countable state space $E = \{k \in \mathbb{Z}_+ : 0 \leq k < N + 1\}$ ($N \leq \infty$). Consider the tridiagonal matrix T or Q as follows:

$$\begin{matrix} T \\ Q \end{matrix} = \begin{pmatrix} -c_0 & b_0 & & & \mathbf{0} \\ a_1 & -c_1 & b_1 & & \\ & a_2 & -c_2 & b_2 & \\ & & \ddots & \ddots & b_{N-1} \\ \mathbf{0} & & & a_N & -c_N \end{pmatrix},$$

where for matrix T : the three sequences $(a_k), (b_k), (c_k)$ are complex; and for (birth-death, abbrev. BD-) matrix Q : the subdiagonal sequences (a_k) and

(b_k) are positive, and the diagonal one satisfies $c_k = a_k + b_k$ for each $k < N$, except $c_N \geq a_N$ if $N < \infty$. For short, we often write T (or Q) $\sim (a_k, -c_k, b_k)$ to denote the tridiagonal matrix. It is well known that the matrix Q possesses the following property:

$$\mu_n a_n = \mu_{n-1} b_{n-1}, \quad 1 \leq n < N + 1 \quad (1)$$

for a positive sequence $(\mu_k)_{k \in E}$. Actually, property (1) is equivalent to

$$\mu_n = \mu_{n-1} \frac{b_{n-1}}{a_n}, \quad 1 \leq n < N + 1 \quad \text{with initial} \quad \mu_0 = 1. \quad (2)$$

In other words, at the present simple situation, one can write down (μ_k) quite easily: starting from $\mu_0 = 1$, and then compute $\{\mu_k\}_{k=1}^N$ step by step (one-step iteration) along the path

$$0 \rightarrow 1 \rightarrow 2 \rightarrow \dots$$

At the moment, it is somehow strange to write T and Q together, since they are rather different. For T , three complex sequences are determined by 6 real sequences and Q is mainly determined by two positive sequences, or equivalently, only one real sequence. However, it will be clear later, these two sequences have some special “blood kinship”, a fact discovered only three years ago [6; §3].

Clearly, for Q , property (1) is equivalent to

$$\mu_i a_{ij} = \mu_j a_{ji}, \quad i, j \in E, \quad (3)$$

provided we re-express the matrix Q as $(a_{ij} : i, j \in E)$ since except the symmetric pair (a_n, b_{n-1}) given in (1), for the other i, j , the equality (3) is trivial. However, for general real $A = (a_{ij} : i, j \in E)$, property (3) is certainly not trivial.

Definition 1 A real matrix $A = (a_{ij} : i, j \in E)$ is called *symmetrizable* if there exists a positive measure $(\mu_k : k \in E)$ such that (3) holds.

The meaning of (3) is as follows. Even though A itself is not symmetric, but once it is evoked by a suitable measure (μ_k) , the new matrix $(\mu_i a_{ij} : i, j \in E)$ becomes symmetric. Every one knows that the symmetry is very important not only in nature, but also in mathematics. Now how far away is it from symmetric matrix to the symmetrizable one. Consider $N = \infty$ in particular. Then symmetry means that $\mu_k \equiv$ a nonzero positive constant, and so as a measure, μ_k can not be normalized as a probability one. Hence, there is no equilibrium statistical physics since for which, the equilibrium measure should be a Gibbs measure (a probability measure). Next, in this case, the most part of stochastics is not useful since the system should die out.

A systemic symmetrizable theory was presented by Hou and Chen in [13] in Chinese (note that it was too hard to obtain necessary references and so

the paper was done without knowing what happened earlier out of China). The English abstract appeared in [14]. Having this tool at hand, our research group was able to go to the equilibrium statistical physics, as shown in [2; Chapters 7, 11 and Section 14.5].

One of the advantage of the symmetric matrix is that it possesses the real spectrum. This is kept for the symmetrizable one. When we go to complex matrix, the symmetric matrix should be replaced by the Hermitian one for keeping the real spectrum. This leads to the following definition.

Definition 2 A complex matrix $A = (a_{ij} : i, j \in E)$ is called *Hermitizable* if there exists a positive measure $(\mu_k : k \in E)$ such that

$$\mu_i a_{ij} = \mu_j \bar{a}_{ji}, \quad i, j \in E, \quad (4)$$

where \bar{a} is the conjugate of a .

Clearly, in parallel to the real case, even though A itself is not Hermitian, but once it is evoked by a suitable measure (μ_k) , the new matrix $(\mu_i a_{ij} : i, j \in E)$ becomes Hermitian. Both A and $(\mu_i a_{ij} : i, j \in E)$ have real spectrum.

From (4), we obtain the following simple result.

Lemma 3 In order the complex $A = (a_{ij})$ to be Hermitizable, the following conditions are necessary.

- The diagonal elements $\{a_{ii}\}$ must be real.
- Co-zero property: $a_{ij} = 0$ iff $a_{ji} = 0$ for all i, j .
- Positive ratio: $\frac{\bar{a}_{ij}}{a_{ji}} = \frac{a_{ij}}{\bar{a}_{ji}} > 0$ or equivalently, positive product: $a_{ij}a_{ji} > 0$.

Proof. The last assertion of the lemma comes from the following identity:

$$\frac{\alpha}{\bar{\beta}} = \frac{\alpha\beta}{|\beta|^2}, \quad \beta \neq 0. \quad \square$$

Combining the lemma with the result on BD-matrix, we obtain the following conclusion.

Theorem 4 (Chen 2018, [6; Corollary 6]) The complex T is Hermitizable iff the following two conditions hold simultaneously.

- (c_k) is real.
- Either $a_{k+1} = 0 = b_k$ or $a_{k+1}b_k > 0$ for each $k: 0 \leq k < N$.

Then, we have

$$\mu_0 = 1, \quad \mu_n = \mu_{n-1} \frac{b_{n-1}}{\bar{a}_n} = \mu_0 \prod_{k=1}^n \frac{b_{k-1}}{\bar{a}_k}.$$

In practice, we often ignore the part “ $a_{k+1} = 0 = b_k$ ” since otherwise, the matrix T can be separated into two independent blocks.

We now come to the general setup. First, we write $i \rightarrow j$ once $a_{ij} \neq 0$. Next, a given path $i_0 \rightarrow i_1 \rightarrow \dots \rightarrow i_n$ is said to be closed if $i_n = i_0$. A closed one is said to be smallest if it contains no-cross or no round-way closed path. A round-way path means $i_0 \rightarrow i_1 \rightarrow i_2 \rightarrow i_1 \rightarrow i_0$ for example. In particular, each closed path for T must be round-way.

Theorem 5 (Chen 2018, [6; Theorem 5]) The complex $A = (a_{ij})$ is Hermitizable iff the following two conditions hold simultaneously.

- *Co-zero property.* For each pair i, j , either $a_{ij} = 0 = a_{ji}$ or $a_{ij}a_{ji} > 0$ (which implies that (a_{kk}) is real).
- *Circle condition.* For each smallest (no-cross-) closed path $i_0 \rightarrow i_1 \rightarrow \dots \rightarrow i_n = i_0$, the circle condition holds

$$a_{i_0 i_1} a_{i_1 i_2} \dots a_{i_{n-1} i_n} = \bar{a}_{i_n i_{n-1}} \dots \bar{a}_{i_2 i_1} \bar{a}_{i_1 i_0}.$$

In words, the product of $a_{i_k i_{k+1}}$ along the path equals to the one of product of $\bar{a}_{i_{k+1} i_k}$ along the inversive direction of the path.

Proof. One may check that our Hermitizability is equivalent to A being Hermitian on the space $L^2(\mu)$ of square-integrable complex function with the standard inner product

$$(f, g) = \int f \bar{g} d\mu.$$

Hence the Hermitizability seems not new for us. However, the author does not know up to now any book tells us how to find out the measure μ . Hence, our main task is to find such a measure if possible. Here we introduce a very natural proof of Theorem 5, which is published here for the first time.

Next, in view of the construction of μ for BD-matrix Q or T , one can find out the measure step by step along a path. We now fix a path as follows.

$$i_0 \rightarrow i_1 \rightarrow \dots \rightarrow i_{n-1} \rightarrow i_n, \quad a_{i_k i_{k+1}} \neq 0.$$

Comparing the jumps and their rates for BD-matrix and the present A :

$$\begin{array}{ll} k-1 \rightarrow k: & b_{k-1}, & i_{k-1} \rightarrow i_k: & a_{i_{k-1} i_k} \\ k \rightarrow k-1: & \bar{a}_k, & i_k \rightarrow i_{k-1}: & \bar{a}_{i_k i_{k-1}}. \end{array}$$

From the iteration for BD-matrix

$$\mu_n = \mu_{n-1} \frac{b_{n-1}}{\bar{a}_n},$$

it follows that for the matrix A along the fixed path above, we should have

$$\mu_{i_n} = \mu_{i_{n-1}} \frac{a_{i_{n-1} i_n}}{\bar{a}_{i_n i_{n-1}}}.$$

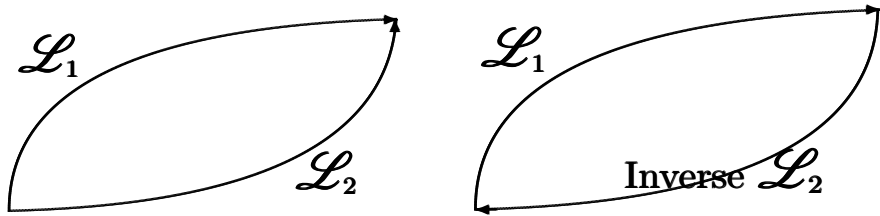
Therefore, we obtain

$$\prod_{k=1}^n \frac{a_{i_{k-1}i_k}}{\bar{a}_{i_k i_{k-1}}} = \frac{\mu_{i_n}}{\mu_{i_0}}. \quad (5)$$

Thus, if we fixed i_0 to be a reference point, then we can compute μ_{i_k} ($k = 1, 2, \dots, n$) successively by using this formula. The essential point appears now, in the present general situation, there may exist several paths from the same $j_0 = i_0$ to the same $j_m = i_n$, as shown in the left figure below. We have to show that along these two paths, we obtain the same $\mu_{i_n} = \mu_{j_m}$. That is the so-called path-independence. This suggests us to use the conservative field theory in analysis. The path-independence is equivalent to the following conclusion: the work done by the field along each closed path equals zero. This was the main idea we adopted in [13]. To see it explicitly, from (5), it follows that

$$w(\mathcal{L}_1) := \sum_{k=1}^n \log \frac{a_{i_{k-1}i_k}}{\bar{a}_{i_k i_{k-1}}} = \log \mu_{i_n} - \log \mu_{i_0}.$$

The left-hand side is the work done by the conservative field along the path \mathcal{L}_1 : $i_0 \rightarrow \dots \rightarrow i_{n-1} \rightarrow i_n$, and the right-hand side is the difference of potential of the field at positions i_n and i_0 . Clearly, once $i_n = i_0$, the right-hand side equals zero (let call it the conservativeness for a moment).



Left figure: Two paths from i_0 to i_n : \mathcal{L}_1 and \mathcal{L}_2 .

Right figure: Combining \mathcal{L}_1 and inverse \mathcal{L}_2 together, we get a closed path.

For the reader's convenience, we check the equivalence of the path-independence

$$w(\mathcal{L}_1) = w(\mathcal{L}_2)$$

and the conservativeness of the field in terms of the right figure

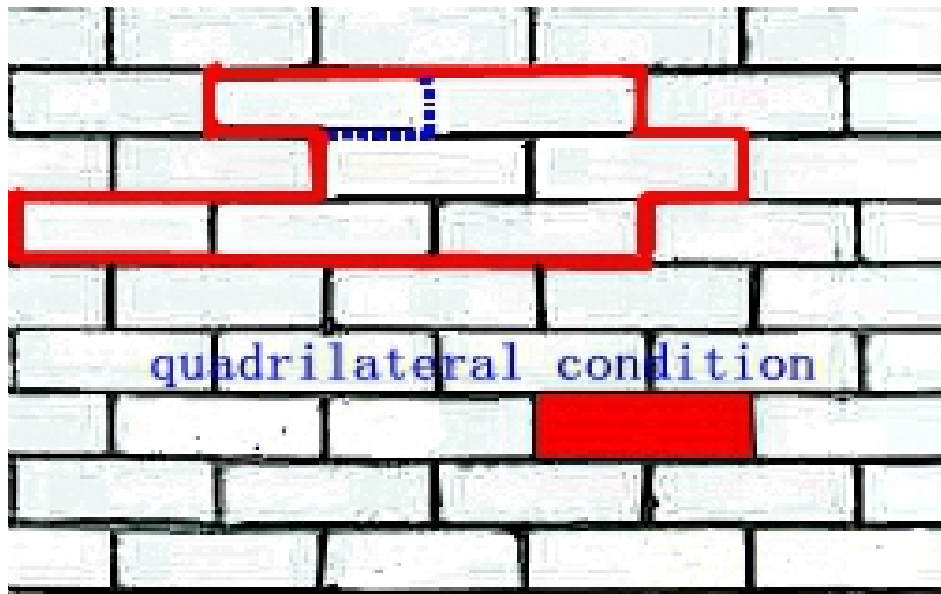
$$w(\mathcal{L}_1) + w(\text{Inverse } \mathcal{L}_2) = 0.$$

The conclusion is obvious by using the third assertion of Lemma 3:

$$w(\text{Inverse } \mathcal{L}_2) = -w(\mathcal{L}_2).$$

The last property is exactly the circle condition given in the theorem, and so the proof is finished. \square

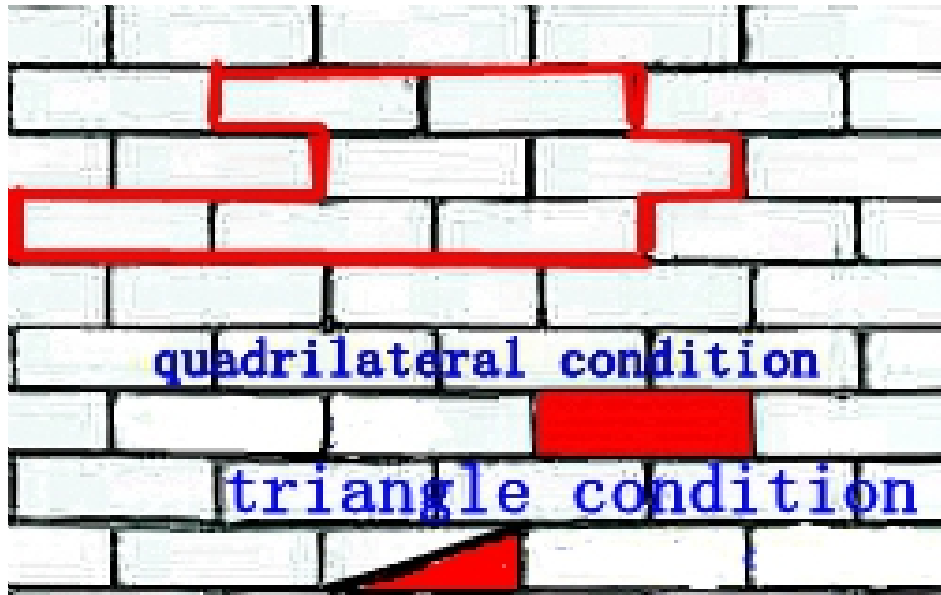
In the special case that A is a transition probability of a finite time-discrete Markov chain, the circle condition was obtained by Kolmogorov [15], as a criterion of the reversibility of the Markov chain. It is also interesting that at the beginning and at the end of [15], the paper by Schrödinger [17] was cited. Moreover, Kolmogorov studied the reversible diffusion in 1937 [16]. These two papers [15, 16] begun the research direction of reversible Markov processes (and also the modern Dirichlet theory). It also indicates the tight relation between the real symmetrizable operators and equilibrium statistical physics. Nevertheless, the interacting subjects “random fields” and “interacting particle systems” were only born in 1960’s. Even though there are some publications along this line, the “Schrödinger diffusion” for instance [1], we are not sure how a distance now to the original aim of Schrödinger who was looking for an equation derived from classical probability, which is as much close as possible to his wave equation in quantum mechanics.



It is regretted that the author had a chance to read [15, 16] only a few years ago when “Selected Works of A.N. Kolmogorov” appeared. Hence, the author did not know anything earlier about Kolmogorov’s [15, 16]. There is a Chinese proverb that says “the ignorant are fearless”. For this reason, we were brave enough to make a restriction “smallest closed path” instead of “every closed one” in the theorem and then we had gone for much far away, since the total number of the closed paths may be infinite, even not countable. To illustrate the idea, let us consider a random chosen wall above. One sees that there are a lot of closed paths. However, the smallest one is quadrilateral. Hence, one has to check only the “quadrilateral condition”. To see this, look at the closed path on the top, and it consists of 7 quadrilaterals. The short path with dash line on the top separates the whole closed path into two smaller

ones. To prove that it sufficient to check the “quadrilateral condition” for this model, we use induction. The idea goes as follows. We can make first the union of these two smaller closed paths (choose the clockwise direction for one of the closed paths and choose anti-clockwise for the other one). Then remove the round-way path with dash line. Thus, once the work done by the field along each of the smaller closed paths equals zero, then so is the one along the original closed path since the work done by the field along the round-way path equals zero.

However, for the second wall below, the smallest closed path, except the quadrilateral, there is also triangle, so we have the “triangle condition”. It is interesting, in [2; Chapters 7 and 11], we use only these two conditions; and in [2; Section 14.5], we use only the triangle condition. The main reason is that for infinite-dimensional objects, their local structures are often regular and simple. Besides, in general we have an algorithm to justify the Hermitizability by computer, refer to [10; Algorithm 1].



We are now arrive at the core part of the paper: describing the spectrum of the Hermitizable matrix, which is also the core part of the so-called matrix mechanics. The next result explains the meaning of “blood kinship” mentioned at the beginning of this section.

Theorem 6 (Chen 2018, [6; Corollary 21]) Up a shift if necessary, each irreducible Hermitizable tridiagonal matrix T is isospectral to a BD-matrix \tilde{Q} which can be expressed by the known sequences (c_k) and $(a_{k+1}b_k)$.

The main condition we need for the above result is $c_k \geq |a_k| + |b_k|$ for every $k \in E$. For finite E , the condition is trivial since one may replace (c_k) by a

shift $(c_k + m)$ for a large enough constant m . For infinite E , one may require this assumption up to a shift.

We now state the construction of $\tilde{Q} \sim (\tilde{a}, -\tilde{c}_k, \tilde{b}_k)$. The essential point is the sequence (\tilde{b}_k) :

$$\tilde{b}_k = c_k - \frac{u_k}{\tilde{b}_{k-1}}, \quad \tilde{b}_0 = c_0,$$

where $u_k := a_k b_{k-1} > 0$. This is one-step iteration, and we have the explicit expression

$$\tilde{b}_k = c_k - \frac{u_k}{c_{k-1} - \frac{u_{k-1}}{c_{k-2} - \frac{u_{k-2}}{\ddots - \frac{u_2}{c_2 - \frac{u_1}{c_1 - \frac{u_1}{c_0}}}}}}.$$

Note that here two sequences (c_k) and (u_k) are explicit known. Having (\tilde{b}_k) at hand, it is easy to write down $\tilde{a}_k = \tilde{c}_k - \tilde{b}_k$ with $\tilde{c}_k = c_k$ for $k < N$, and $\tilde{a}_N = u_N/\tilde{b}_N$ if $N < \infty$. The solution of (\tilde{a}_k) and (\tilde{c}_k) are automatic so that \tilde{Q} becomes a BD-matrix.

The resulting matrix \tilde{Q} looks very simple, but it contains a deep intrinsic feature. For instance, the reason is not obvious why the sequences (\tilde{b}_k) and (\tilde{a}_k) are positive even though so are (c_k) and (u_k) . With simple description but deep intrinsic feature is indeed a characteristic of a good mathematical result.

To see the importance of the above theorem, let compare the difference of the principal eigenvector of these two matrices. First, for BD-matrix with four different boundaries, the principal eigenvectors are all monotone, except in one case, it is concave. This enables us to obtain a quite satisfactory theory of the principal eigenvalues (refer to [4]). However, since the Hermitizable T has real spectrum, from the eigenequation

$$Tg = \lambda g,$$

one sees immediately, the eigenvector g must be complex, too far away to be monotone. Thus, the principal eigenvectors of these two operators are essentially different. It shows that we now have a new spectral theory for the Hermitizable tridiagonal matrices.

Because the intuition is not so clear why Theorem 6 should be true, two alternative proofs are presented in [7].

Theorem 7 (Chen 2018, [6; Theorem 24]) The spectrum of a finite Hermitizable matrix A is equal to the union of the spectrums of m BD-matrices, where m is the largest multiplicity of eigenvalues of A .

Refer to [10; Proofs in §4] for details. The proof is based on Theorem 6 and the “Householder transformation” which is one of the 10 top algorithms in the twentieth century. The restriction to the finite matrix is due to the use of the transformation. The number m is newly added here which comes from the fact that the eigenvalues of BD-matrices must be distinct and simple, as illustrated by [10; Example 9].

Theorem 7 provides us a new architecture for the study on matrix mechanics (and then for quantum mechanics) since we have a unified setup (BD-matrix) to describe its spectrum. This leads clearly to a new spectrum theory, as illustrated by [7] for tridiagonal matrix and by [11] for one-dimensional diffusions. It also leads to some new algorithms for computational mathematics, as illustrated by [10, 9].

2 Hermitizable, isospectral differential operators

Two approaches for studying the Schrödinger operator

- 1) The most popular approach to study the Schrödinger operator

$$L = \frac{1}{2}\Delta + V$$

is the Feynman-Kac semigroup $\{T_t\}_{t \geq 0}$:

$$T_t f(x) = \mathbb{E}_x \left\{ f(w_t) \exp \left[\int_0^t V(w_s) ds \right] \right\},$$

where (w_t) is the standard Brownian motion. This is often an unbounded semigroup. The Schrödinger operator was born for quantum mechanics, and it is 95 years older this year. In the past hundred years or so, there are a huge number of publications devoted to the operator. However, for the discrete spectrum which is the most important problem in quantum mechanics, the useful results are still very limited as far as we know. In particular, even in dimension one, we have not seen the results which are comparable with [5].

- 2) As in the first section, this paper introduces a new method to study the spectrum of Schrödinger operator. That is, replacing the operator L above by

$$\tilde{L} = \frac{1}{2}\Delta + \tilde{b}^h \nabla,$$

where h is a harmonic function: $Lh = 0$, $h \neq 0$ (a.e.). Then, the operator L on $L^2(dx)$ is isospectral to the operator \tilde{L} on $L^2(\tilde{\mu}) := L^2(|h|^2 dx)$.

We now consider a general operator. Let $a_{ij}, b_i, c : \mathbb{R}^d \rightarrow \mathbb{C}$, $V : \mathbb{R}^d \rightarrow \mathbb{R}$, and set $a = (a_{ij})_{i,j=1}^d$, $b = (b_i)_{i=1}^d$. Define $d\mu = e^V dx$ and

$$L = \nabla(a\nabla) + b \cdot \nabla - c.$$

Here is the result on the Hermitizability. Denote by a^H the transpose (a^*) and conjugate (\bar{a}) of the matrix a .

Theorem 8 (Chen and Li 2020 [11]) Under the Dirichlet boundary condition, the operator L is Hermitizable with respect to μ iff $a^H = a$ and

$$\begin{aligned} \operatorname{Re} b &= (\operatorname{Re} a)(\nabla V), \\ 2 \operatorname{Im} c &= -((\nabla V)^* + \nabla^*)((\operatorname{Im} a)(\nabla V) + \operatorname{Im} b). \end{aligned}$$

Recall that a key point in the isospectral transform of T and \tilde{Q} is that the resulting matrix \tilde{Q} obeys the condition $\tilde{c}_k = \tilde{a}_k + \tilde{b}_k$ for each $k < N$, and there is no killing/potential term at the diagonal (maybe except only one at the endpoint if $N < \infty$). In the next result, we also remove the potential term c in L .

Theorem 9 (Chen and Li 2020 [11]) Denote by $\mathcal{D}(L)$ the domain of L on $L^2(\mu)$ and let h be harmonic: $Lh = 0$, $h \neq 0$ (a.e.). Then $(L, \mathcal{D}(L))$ is isospectral to the operator $(\tilde{L}, \mathcal{D}(\tilde{L}))$:

$$\begin{cases} \tilde{L} = \nabla(a\nabla) + \tilde{b} \cdot \nabla, \\ \mathcal{D}(\tilde{L}) = \{\tilde{f} \in L^2(\tilde{\mu}) : \tilde{f}h \in \mathcal{D}(L)\}; \end{cases}$$

where

$$\tilde{b} = b + 2 \operatorname{Re}(a) \mathbb{1}_{[h \neq 0]} \frac{\nabla h}{h}, \quad \tilde{\mu} := |h|^2 \mu.$$

The discrete spectrum for one-dimensional elliptic differential operator is also illustrated in [11]. Certainly, much of the research work should be done in the near future. For instance, Hermitizable operator is clearly the Hermitian operator on the complex space $L^2(\mu)$. It naturally corresponds to a Dirichlet form. Hence there should be a complex process corresponding to the operator. It seems that this is still a quite open area, except a few of papers, Fukushima and Okada [12] for instance.

In conclusion, the paper [13] published 42 years ago opened a door for us to go to the equilibrium/nonequilibrium statistical physics (cf. [2, 3]); the paper [6] that appeared 3 years ago enables us to go to quantum mechanics. The motivation of the present study from quantum mechanics was presented in details in [8] but omitted here.

Acknowledgement: This study is supported by the National Natural Science Foundation of China (Project No.: 12090011), National key R & D plan (No. 2020Y-FA0712900). Supported by the “double first class” construction project of the Ministry of education (Beijing Normal University) and the advantageous discipline construction project of Jiangsu Universities. It is an honor to the author to contribute the paper to the Festschrift in honor of Masatoshi Fukushimas Beiju.

References

- [1] Aebi, R. (1996). *Schrödinger Diffusion Processes*. Birkhäuser Verlag.
- [2] Chen, M.F. (2004). *From Markov Chains to Nonequilibrium Particle Systems*, 2nd ed. World Sci, Singapore.
- [3] Chen, M.F. (2005). *Eigenvalues, Inequalities, and Ergodic Theory*. Springer.
- [4] Chen, M.F. (2010). *Speed of stability for birth–death processes*. *Front. Math. China* 5(3): 379–515.
- [5] Chen, M.F. (2011). Basic estimates of stability rate for one-dimensional diffusions, Chapter 6 in “Probability Approximations and Beyond”, pp. 75–99. *Lecture Notes in Statistics 205*, Editors: Andrew Barbour, Hock Peng Chan, David Siegmund.
- [6] Chen M.F. (2018). *Hermitizable, isospectral complex matrices or differential operators*. *Front Math China* 13(6): 1267–1311.
- [7] Chen M.F. (2020). *On spectrum of Hermitizable tridiagonal matrices*. *Front. Math. China* 15(2): 285–303.
- [8] Chen M.F. (2021). *A New Mathematical Perspective of Quantum Mechanics* (In Chinese). *Adv. in Math. (China)* 50(3): 321–334.
- [9] Chen M.F., Chen, R.R (2021). *Top eigenpairs of large dimensional matrix*. *SIAM Trans. Appl. Math.* 3(1): 1–25.
- [10] Chen, M.F., Jia, Z.G., Pang, H.K. (2021). *Computing top eigenpairs of Hermitizable matrix*. *Front. Math. China*.
- [11] Chen, M.F. and Li, J.Y. (2020). *Hermitizable, isospectral complex second-order differential operators*. *Front. Math. China* 15(5): 867–889.
- [12] Fukushima, M. and Okada, M. (1987). *On Dirichlet forms for plurisubharmonic functions*. *Acta Math.* 159, Issue 1, 171–213.
- [13] Hou, Z.T. and Chen, M.F. (1979). Markov processes and field theory. Chapter 6 in “Reversible Markov Processes” (in Chinese), edited by M. Qian and Z. T. Hou. pages 194–242. Hunan Sci. Press.
- [14] Hou, Z.T. and Chen, M.F. (1980). *Markov Processes and field theory* (Abstract) *Kuoxue Tongbao* 25 (10): 807–811.
- [15] Kolmogorov, A.N. (1936). *Zur Theorie der Markoffschen Ketten*. *Math. Ann.*, 112: 155–160. English translation: On the theory of Markov chains. Article 21 in *Selected Works of A.N. Kolmogorov*, Vol. II: Probability Theory and Mathematical Statistics, 182–187, edited by A.N. Shiriyayev. Nauka, Moscow 1986. Translated by G. Undquist. Springer 1992.
- [16] Kolmogorov, A.N. (1937). *Zur Umkehrbarkeit der statistischen Naturgesetze*. *Math. Ann.* 113: 766–772. English translation: On the reversibility of the statistical laws of nature. Article 24 in “Selected Works of A.N. Kolmogorov”, Vol. II: 209–215.
- [17] Schrödinger, E. (1931). *Über die Umkehrung der Naturgesetze*. *Sitzungsber. Preuss. Akad. Wiss., Phys.-Math. Kl.*, 12 März. 144–153.

Mailing Address:

1 Research Institute of Mathematical Science, Jiangsu Normal University. Shanghai Lu 101, Tongshan Xinqu, Xuzhou, Postcode: 221116.

2 Key Laboratory of Mathematics and Complex System, School of Mathematical Sciences, Beijing Normal University. Beijing, Postcode: 100875.

E-mail: mfchen at bnu dot edu dot cn **Home Page:** <http://math0.bnu.edu.cn/~chenmf>